Towards a Better (Litho-) Stratigraphy and Reconstruction of Quaternary Paleoenvironment in the Amerasian Basin (Arctic Ocean)

by Ruediger Stein[1], Jens Matthiessen[1], Frank Niessen[1], Alexey Krylov[2], Seung-il Nam[3] and Evgenia Bazhenova[1,4]

Abstract: New sediment cores were recovered along two transects from the Canada Basin across the central Mendeleev Ridge towards the Makarov Basin and the Lomonosov Ridge in the Eurasian Arctic (northern transect along 80°30' N, southern transect along 77°30' N). Here, we present first results from RV "Polarstern" ARK-XXIII/3 expedition (August-October 2008). Based on the visual core description, Clark's standard lithological units A to M (CLARK et al. 1980) could also be clearly identified in sediment cores from the northern transect across Mendeleev Ridge. The content of sand-sized material, the prominent pink-white layers, and – especially in the upper part of the records – the distinct brown/beige colour cycles were considered to be the key sedimentary characteristics used for core correlation and for establishing a tentative age model.

Based on this age model, the sediments recovered in cores from the southern transect are younger than Marine Isotope Stage (MIS) 8, whereas the cores from the northern transect also contain sediments probably significantly older than MIS 16. Average sedimentation rates for the time interval MIS 1 to 5 in cores from the northern transect reach values of 0.5-0.9 cm ky^{-1} (top Mendeleev Ridge and Canadian side), increasing to 1.9-2.4 cm ky^{-1} at the Makarov Basin side. Along the southern transect, sedimentation rates are significantly higher, reaching 4.2 to >6 cm ky^{-1}.

The most distinct pinkish intervals characterized by high numbers of dolomitic ice-rafted debris (IRD) are related to increased IRD supply due to disintegration of an extended Laurentide Ice Sheet during MIS 8(/7), MIS 5d, and MIS 4/MIS 3. The sand-rich intervals and detrital-carbonate maxima found in the deeper part of the sediment sections from the northern transect may reflect events of IRD input due to disintegration events of the Laurentide Ice Sheet at the end of glacial MIS 8, 10, 12, and 16, a still speculative hypothesis that has to be approved by further studies.

A diamicton with erosional structures at its base was identified on southern Mendeleev Ridge in water depths of 800-900 m, suggesting the impact of grounding ice masses during a glaciation older than MIS 5a.

Future research of this unique new core material recovered during the "Polarstern" expedition may help to answer key questions in Arctic Ocean stratigraphy/chronology to unravel the history of circum-Arctic glaciations.

Zusammenfassung: Während der Expedition ARK-XXIII/3 von FS "Polarstern" (August-Oktober 2008) wurden Sedimentkerne auf zwei Transekten entlang 80°30' N und 77°30' N vom Kanada-Becken über den zentralen Mendeleev-Rücken bis in das Makarov-Becken gewonnen. Die von CLARK et al. (1980) für das Amerasische Becken aufgestellte Standard-Lithostratigraphie mit den Standard-Einheiten A bis M konnte auch in den neuen Kernen vom nördlichen Transekt eindeutig nachgewiesen werden. Die Gehalte an Sandfraktion, charakteristische "pink-white layers" und – insbesondere im oberen Teil der Abfolgen – markante (dunkel-)braune Intervalle sind Grundlage für die Korrelation der Kerne und die Erstellung eines vorläufigen Altersmodells. Basierend auf diesem Altersmodell sind die Sedimente der Kerne vom südlichen Transekt wahrscheinlich nicht älter als das Marine Isotopen-Stadium (MIS) 8, während die Sedimente vom nördlichen Transekt z.T. deutlich älter als MIS 16 sind. Die mittleren Sedimentationsraten erreichen auf

dem nördlichen Transekt 0.5-0.9 cm ky^{-1} (Top Mendeleev-Rücken und Kanada-Becken) und 1.9-2.4 cm ky^{-1} (Makarov-Becken). Auf dem südlichen Transekt dagegen sind die mittleren Sedimentationsraten mit 4.2->6 cm ky^{-1} deutlich höher. Die markanten, durch hohe Anteile an Dolomit-reicher Grobfraktion gekennzeichneten "pink-white layers" werden mit einem erhöhten Eintrag von durch Eisberge transportiertem Material erklärt, der auf den Zerfall des ausgedehnten Laurentischen Eisschildes während MIS 8 (/7), MIS 5d bzw. MIS 4/MIS 3 zurückgeführt wird. Die Sand- und Dolomit-reichen Lagen aus tieferen Kernabschnitten mögen auf ähnliche Ereignisse während der Kaltstadien MIS 10, 12 und 16 hinweisen, eine Hypothese, die durch weitere Untersuchungen bestätigt werden muss. Auf dem südlichen Mendeleev-Rücken ist in sedimentakustischen Aufnahmen ein Diamikt mit Erosionsstrukturen an der Basis zu erkennen, der auf Erosion durch ein aufsitzendes größeres Eismassiv hinweisen könnte.

INTRODUCTION

Paleoclimate research and climate models demonstrate that processes and varying conditions in the High Northern Latitudes play a key role in driving and amplifying global climate variability and sea-level change on time scales of decades to millions of years (e.g., SERREZE et al. 2000, ACIA 2005, IPCC 2007). Despite of the importance of the Arctic Ocean in the global climate system, the knowledge of its short- and long-term paleoceanographic and paleoclimatic history is much behind that from other world ocean areas. This lack of knowledge is mainly caused by the major technological and /or logistical problems in reaching this permanently ice-covered region with regular research vessels and in retrieving long and undisturbed sediment cores. High-resolution records dealing with the late Quaternary history of circum-Arctic ice sheets and its relationship to the paleoceanographic circulation pattern in the central Arctic Ocean, for example, are still limited and are/were in the focus of several international multidisciplinary research projects and related expeditions carried-out during the last two decades, e.g., the expedition of „Polarstern" and „Oden" in 1991 (FÜTTERER 1992), the „Polar Sea" expedition in 1993 (GRANTZ et al. 1998), the expedition of „Louis St. Laurent" and „Polar Sea" in 1994 (WHEELER 1997), the expeditions of „Oden" in 1996 and 2007 (BACKMAN et al. 1997, JAKOBSSON et al. 2007), the expeditions of „Polarstern"in 1998, 2004, and 2007 (JOKAT et al. 1999, STEIN 2005, SCHAUER, 2008), and the expedition of „Healy" and „Oden" in 2005 (DARBY et al. 2005). In this context, the very recent expedition of „Polarstern" (ARK-XXIII/3) in 2008 (JOKAT 2009) has to be listed as well.

Based on available Late Quaternary sedimentary records from the Canada Basin and the Mendeleev Ridge, major glaciations

in North America probably occurred during Marine Isotope Stage (MIS) 6, MIS 5d, near the boundary between MIS 4 and MIS 3 (MIS 4/3), and during the Last Glacial Maximum (LGM) (Fig. 1; e.g., POLYAK et al. 2004, DARBY et al. 2006). Unfortunately, the pre-LGM history of North American (Laurentide) glaciations is still poorly understood in detail (POLYAK et al. 2007). Records from the Eurasian Basin, on the other hand, indicate major glaciations in Eurasia during MIS 6, MIS 5b, near the boundary of MIS 5/4 and 4/3, and during the LGM (Fig. 1; e.g., KNIES et al. 2000, 2001, SPIELHAGEN et al. 2004), which correlates quite well with land records (SVENDSEN et al. 2004). Up to now, it cannot be definitely decided whether these differences reflect a (partly) asynchronous evolution of circum-Arctic ice sheets or whether it is just due to missing good-quality data sets across the entire central Arctic Ocean. Traces for glaciations in eastern Siberia are available from land records (Fig. 1; EHLERS & GIBBARD 2007 and references therein). The exact timing of major glaciations in East Siberia, however, is virtually unknown until now due to missing marine sedimentary records from the East Siberian continental margin. A widespread intra-MIS 5 glaciation in the Beringia region has been proposed by BRIGHAM-GRETTE et al. (2001).

The history of circum-Arctic glaciations is also paralleled by distinct changes in central Arctic Ocean paleoenvironment such as the variability of sea-ice cover, surface-water productivity, and paleoceanographic circulation patterns. The latter includes the development of the Beaufort Gyre and Transpolar Drift System, the two main surface-water current systems in the Arctic Ocean (Fig. 2; e.g., MACDONALD et al. 2003). These current systems are important for the transport of terrigenous sediments from the surrounding continents into the central Arctic Ocean. Since the geology of the hinterland is quite different from region to region, specific mineralogical and/or geochemical tracers (e.g., clay and heavy minerals, iron-oxid grains, and minor and major elements) can be used to identify source regions and transport pathways of the terrigenous sediment fractions in Arctic Ocean sediment cores (Fig. 2; NÜRNBERG et al. 1994, STEIN et al. 1994a, BISCHOF & DARBY 1997, VOGT 1997, SPIELHAGEN et al. 1997, NØRGAARD-PEDERSEN et al. 1998, 2007b, WAHSNER et al. 1999, PHILLIPS & GRANTZ 2001, DARBY 2003, VISCOSI-SHIRLEY et al. 2003, POLYAK et al. 2004, ENGLAND et al. 2009, STEIN 2008 for synthesis and references). Thus, these data may give important information about both past glaciations on the continent as well as the intensity and location of the Beaufort Gyre and Transpolar Drift systems.

From recent observations it is known that intensity and location of the Arctic surface-water circulation systems are related to the variability of the atmospheric Arctic Oscillation (AO) and North Atlantic Oscillation (NAO) systems (HURRELL 1995, PROSHUTINSKY & JOHNSON 1997, THOMPSON & WALLACE 1998, DICKSON et al. 2000). Thus, a multi-proxy approach to study changes of the Beaufort Gyre and Transpolar Drift System in quite detail may also give important information about past changes in the NAO/AO systems, which is of major significance for the (global) climate system (e.g., DARBY et al. 2002, DARBY & BISCHOF 2004).

In this context, the overall goal of the geology programme of "Polarstern" ARK-XXIII/3 expedition was to obtain high-quality sediment cores for a multi-proxy study and correlation of sedimentary sections on transects across the central Arctic Ocean from the Canada Basin to the Eurasian Basin in order to (i) develop a stratigraphical and chronological framework as precise as possible and (ii) answer the following key questions
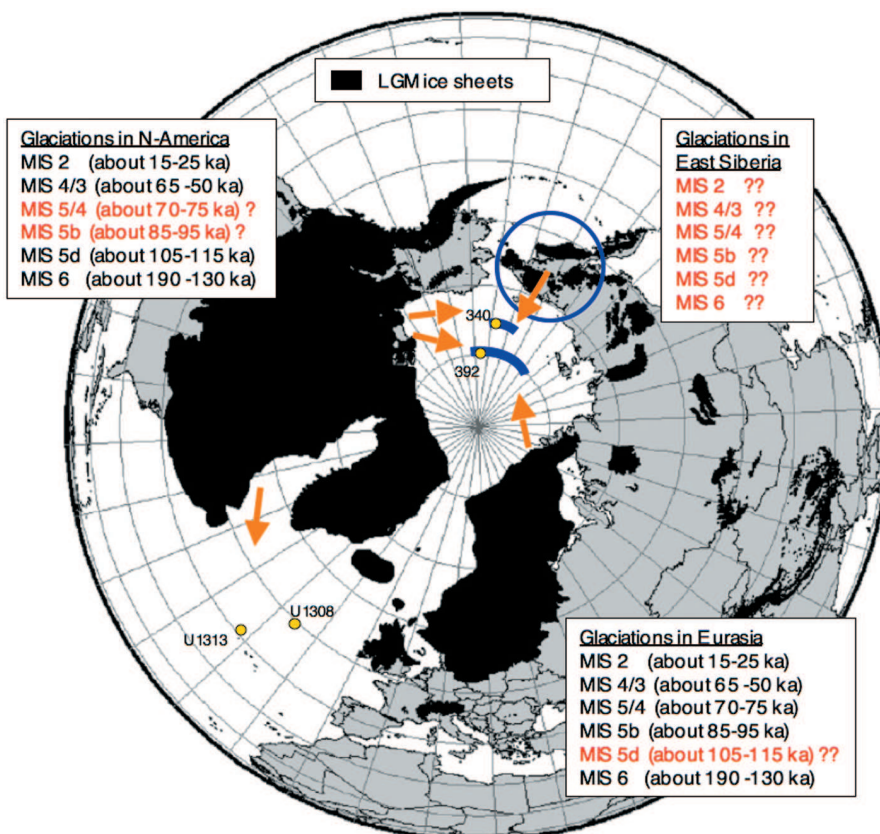

Fig. 1: Extent of Last Glacial Maximum (LGM) glaciation in the Northern Hemisphere (from EHLERS & GIBBARD 2007, supplemented). Proposed ages of major late Quaternary circum-Arctic glaciations are listed (MIS = Marine Isotope Stage, ka = thousand years before present). For several intervals, the timing of glaciations, especially in East Siberia, is still under discussion.
Orange arrows indicate sediment discharge by icebergs. Blue lines mark main transects sampled during "Polarstern" ARK-XXIII/3 expedition, locations of sediment cores PS72/340 and PS72/392 are indicated. U1308 and U1313 mark locations of IODP sites in the North Atlantic (CHANNEL et al. 2006, STEIN et al. 2009a).

Abb. 1: Verbreitung der nordpolaren Eisschilde während des Letzten Glazialen Maximums (LGM) (ergänzt nach EHLERS & GIBBARD 2007). Weitere spätquartäre Vereisungsphasen in Nordamerika, Eurasien und Ostsibirien sind aufgeführt (MIS = Marines Isotopenstadium, ka = 1000 Jahre vor heute).
Orange Pfeile = Sedimenteintrag über Eisberge, blaue Linien = Lage der Beprobungsprofile während "Polarstern" ARK-XXIII/3. Die Positionen der Kerne PS72/340 und PS72/392 (diese Arbeit) sowie der IODP-Kerne U1308 und U1313 im Nordatlantik (CHANNEL et al. 2006, STEIN et al. 2009a) sind markiert.
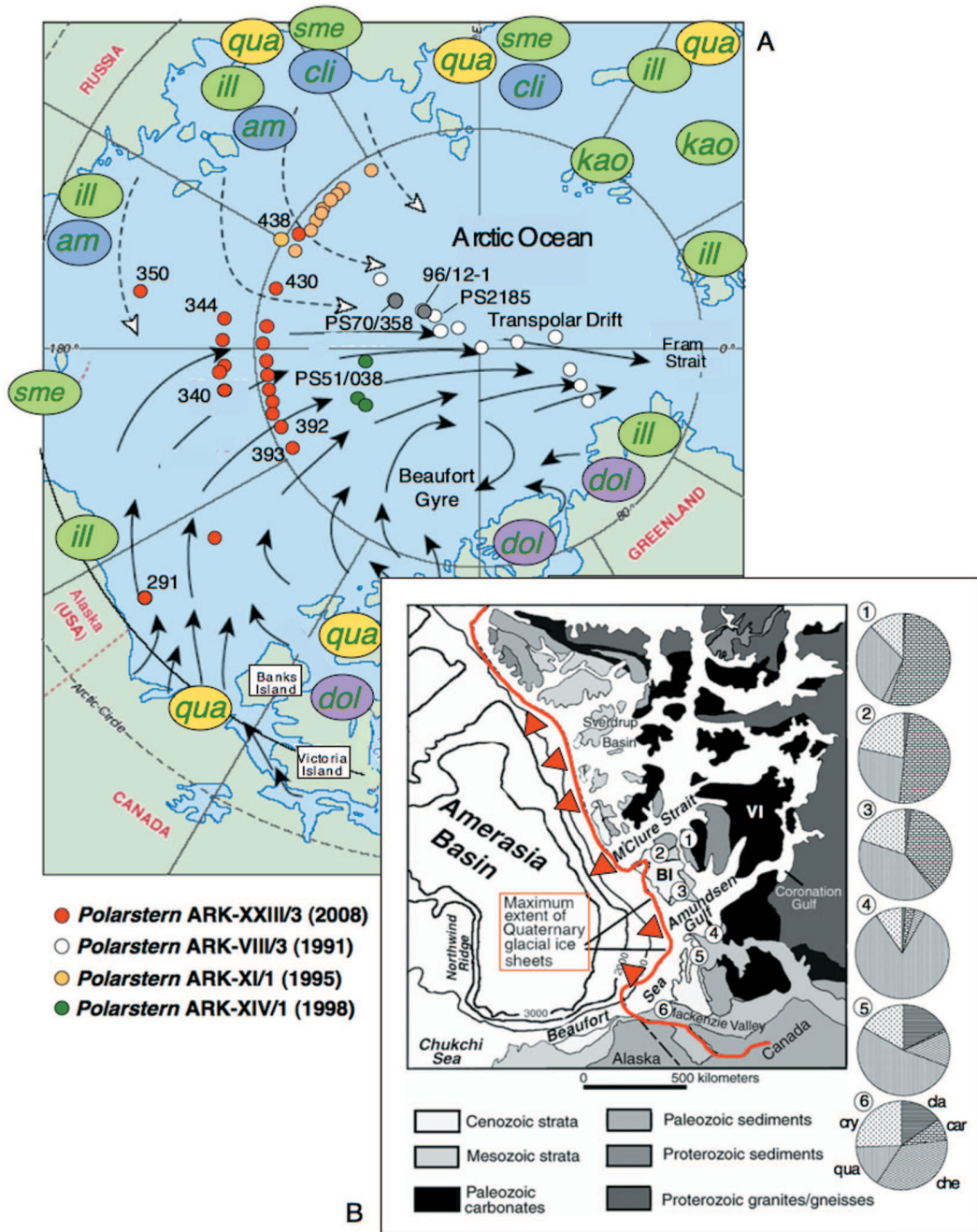
Fig. 2: (A) Map of the inferred iceberg drift directions from North American sources (solid arrows) and hypothesized drift of Siberian pack ice (broken arrows) during glacial intervals (from STOKES et al. 2005, based on BISCHOF & DARBY 1997 and PHILLIPS & GRANTZ 2001, supplemented). As proposed by these authors, the sea-ice drift in the western Arctic Ocean was mostly similar to the iceberg drift, but sea ice occasionally drifted from Siberian sources into the western Arctic Ocean along paths shown as shaded broken arrows. Main source areas of specific minerals are indicated: ill = illite, kao = kaolinite, sme = smectite, am = amphibole, cli = clinopyroxene, qua = quartz, dol = dolomite (based on STEIN et al. 1994a, VOGT 1997, BEHRENDS 1999, WAHSNER et al. 1999, PHILLIPS & GRANTZ 2001, STEIN 2008).
Locations of cores from "Polarstern" ARK-XXIII/3 expedition (JOKAT 2009) and selected cores from "Polarstern" expeditions ARK-VIII/3 (FÜTTERER 1992), ARK-XI/1 (RACHOR 1997), and ARK-XIV/1 (JOKAT 1999) are indicated. Numbers of cores discussed in the text are shown (cores PS51/038, PS2185, PS70/358, 96/12-1pc; cores 291, 340, etc. = cores PS72/291, PS72/340, etc.).
(B) Generalized geological map of the Canadian Arctic Islands, north-western Canada and Alaska with maximum Pleistocene glacial ice edge (red line) and sediment input by major glacier ice streams (red triangles) (from PHILLIPS & GRANTZ 2001, supplemented). In addition, the mineralogical composition of till samples (grain percent of >250 µm fraction) from the Canadian Arctic are shown. Locations and diagrams 1 to 6; cla = clastics, car = carbonate, che = chert, qua = quartz, cry = crystalline (data from Bischof et al. 1996, figure from STEIN 2008).

Abb. 2: (A) Karte der angenommenen Drift-Routen von Eisbergen mit nordamerikanischer Herkunft (volle Pfeile) und mit sibirischer Herkunft (offene Pfeile) während der Glazialphasen (ergänzt nach STOKES et al. 2005, basierend auf BISCHOF & DARBY 1997 und PHILLIPS & GRANTZ 2001). Zusätzlich sind potentielle Liefergebiete bestimmter Minerale dargestellt: ill = Illit, kao = Kaolinit, sme = Smektit, am = Amphibol, cli = Clinopyroxen, qua = Quarz, dol = Dolomit (nach STEIN et al. 1994a, VOGT 1997, BEHRENDS 1999, WAHSNER et al. 1999, PHILLIPS & GRANTZ 2001, STEIN 2008). Positionen der Kerne von "Polarstern"-Expedition ARK-XXIII/3 (JOKAT 2009) und ausgesuchter Kerne der Expeditionen ARK-VIII/3 (FÜTTERER 1992), ARK-XI/1 (RACHOR 1997) und ARK-XIV/1 (JOKAT 1999) sind eingetragen. Nummern von Kernen, die im Text diskutiert werden, sind markiert (Kerne PS51/038, PS2185, PS70/358, 96/12-1pc, Kerne 291, 340, etc. = Kerne PS72/291, PS72/340, etc.).
(B) Vereinfachte geologische Karte des kanadischen Archipels, Nordwest-Kanada und Alaska mit maximaler pleistozäner Verbreitung kontinentaler Eismassen (rote Linie) und Sedimenteintrag durch glazigene Eisströme (rote Dreiecke) (ergänzt nach PHILLIPS & GRANTZ 2001). Zusätzlich sind die Mineralvergesellschaftungen der Kornfraktion >250 µm von Geschiebe-Proben aus der kanadischen Arktis dargestellt. 1 bis 6 = Proben-Lokationen und Diagramme, cla = Klastika, car = Karbonat, che = Feuerstein, qua = Quarz, cry = kristalline Gesteinsbrocken. (Daten nach BISCHOF et al. 1996, Abbildung nach STEIN 2008).
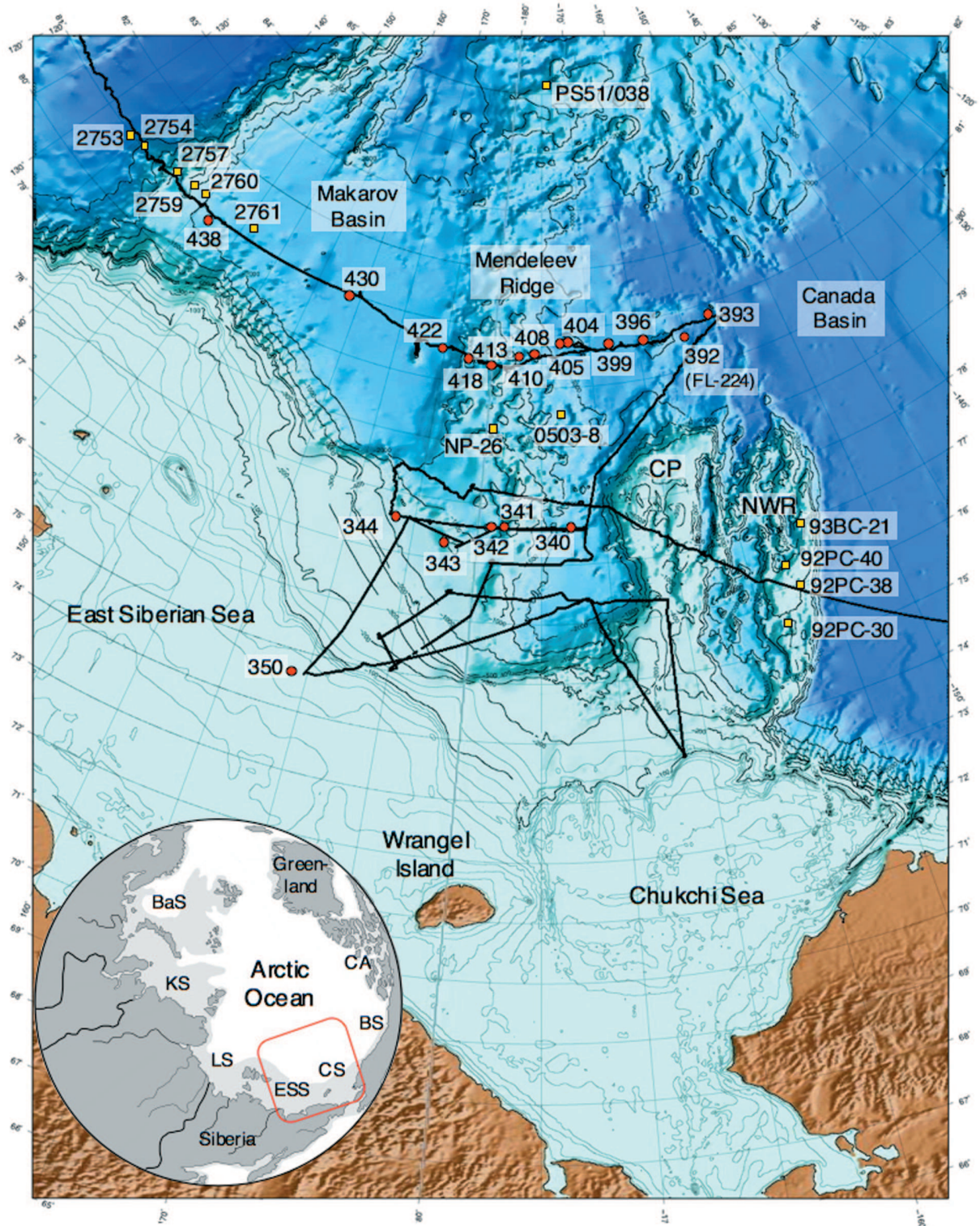
Fig. 3: Map of cruise track and sampling locations (red circles) of "Polarstern" ARK-XXIII/3 expedition (340 = PS72/340, 341 = PS72/341, etc.). Core PS72/392-5 is a re-coring at the location of Clark's key core FL-224 (Clark et al. 1980; for details see Stein et al. 2009, this vol.). Yellow squares = locations of cores NP-26 and 0503-8 (= HLY0503-8JPC; POLYAK et al. 2004, 2009), Northwind Ridge cores 92PC-30, 92PC-38, 92PC-40, and 93BC-21 (PHILLIPS & GRANTZ 2001), Alpha Ridge core PS51/038 (JOKAT 1999) and Lomonosov Ridge cores PS2753-2, PS2754-8, PS2757-8, PS2759-8, PS2760-6, and PS2761-10 (RACHOR 1997); CP = Chukchi Plateau; NWR = Northwind Ridge. Inlay map shows study area within the Arctic Ocean: ESS = East Siberian Sea, CS = Chukchi Sea, BS = Beaufort Sea, CA = Canadian Archipelago, BaS = Barents Sea, KS = Kara Sea, LS = Laptev Sea.

Abb. 3: Karte mit Fahrt-Route und Lokationen der geologischen Stationen während "Polarstern"-Expedition ARK-XXIII/3 (rote Punkte; 340 = PS72/340, 341 = PS72/341, etc.). Kern PS72/392-5 wurde an derselben Position wie Clark's Schlüsselkern FL-224 (CLARK et al. 1980) gezogen. Weiterhin sind Lokationen der Kerne NP-26 and 0503-8 (= HLY0503-8JPC; POLYAK et al. 2004, 2009), der Kerne 92PC-30, 92PC-38, 92PC-40 und 93BC-21 vom Northwind-Rücken (PHILLIPS & GRANTZ 2001), vom Alpha-Rücken PS51/038 (Jokat 1999) und Lomonosov-Rücken PS2753-2, PS2754-8, PS2757-8, PS2759-8, PS2760-6, und PS2761-10 (RACHOR 1997) angezeigt (gelbe Quadrate). CP = Chukchi-Plateau; NWR = Northwind-Rücken. Die Indexkarte zeigt das Arbeitsgebiet (rot umrandet) im Arktischen Ozean: ESS = Ostsibirische See, CS = Chukchisee, BS = Beaufortsee, CA = Kanadischer Archipel, BaS = Barentssee, KS = Karasee, LS = Laptewsee.

related to paleoenvironmental change:
(a) What is the Quaternary history of circum-Arctic ice sheets? Did extensive late Quaternary circum-Arctic ice sheets developed synchronously or asynchronously in North America, North Greenland, East Siberia, and Eurasia?
(b) How did the major surface-water current systems (Beaufort Gyre and Transpolar Drift System) evolve and change in space and time?
(c) How did the sea-ice cover, surface-water productivity, and inflow of Pacific waters through Bering Strait change in time and space?

During the "Polarstern" ARK-XXIII/3 expedition in August through October 2008, new sediment cores were recovered on two transects from the Canadian Arctic across the central Mendeleev Ridge towards the Makarov Basin and the Lomonosov Ridge in the Eurasian Arctic (Fig. 3; JOKAT 2009, STEIN et al. 2009b).

One of these cores (PS72/392-5) is a re-coring at the site of Clark's key core FL-224 (CLARK et al. 1980; see Fig. 3 for location). This will allow on the one hand to identify and to approve Clark's lithostratigraphy and, on the other hand, to use up-to-date tools and methods in paleoceanography needed for a precise core correlation, a development of a more accurate age model, and a more detailed reconstruction of paleoenvironmental history (see also STEIN et al. this vol.). Together with other sediment cores recovered during previous "Polarstern" expeditions, unique core material from several transects crossing the entire central Arctic Ocean is now available for future research (Fig. 2). In this paper, we present first results and interpretation based mainly on shipboard data.

STRATIGRAPHY IN THE AMERASIAN BASIN: BACKGROUND, PROBLEMS, AND PERSPECTIVES

For the interpretation of geological records in terms of paleoenvironmental changes versus time, a reliable stratigraphical (chronological) framework is necessary. This framework may be based on AMS^{14}C datings, oxygen isotope stratigraphy, magneto-stratigraphy, biostratigraphy, lithostratigraphy, and logging records. These dating techniques are routinely used in studies from most world ocean areas. For Arctic Ocean sediments, however, several problems are obvious resulting in difficulties in establishing accurate age-depth relationships in the existing sediment cores (see BACKMAN et al. 2004 cum lit.). Poor preservation of calcareous and biosiliceous microfossil faunas and floras in Arctic sediment cores and strong freshwater discharge into the Arctic Ocean influencing oxygen isotope variability, for example, often precludes application of conventional biostratigraphic and isotopic dating techniques. These difficulties in Arctic Ocean stratigraphy may explain why over decades, there has been a long-lasting and still ongoing controversial discussion whether the central Arctic Ocean sediments were deposited under a senario characterized by very low sedimentation rates of about 0.04 to 0.4 cm ky^{-1} or a senario characterized by significantly higher sedimentation rates of about one to a few cm ky^{-1} (BACKMAN et al. 2004).

For the Amerasian Basin, CLARK et al. (1980) developed a widely accepted standard lithostratigraphy based on a detailed sedimentological study of several hundreds of short sediment cores collected from Ice Island T-3 in the Amerasian Basin between 1952 and 1974. These authors established 13 standard lithostratigraphic (SL) units A to M, which include silty and arenaceous lutites, and carbonate-rich, pinkish-white layers, with variable characteristic contents of quartz-feldspar, detrital carbonate grains, foraminifers, and Fe-Mn particles (see Fig. 2 in STEIN et al. this vol.). The content of sand-sized material (enriched in SL units C, F, H, J, L, and parts of M) and the pink-white layers were considered the key sedimentary characteristics used for correlation of these lithostratigraphic units. At cores from the Alpha Ridge, Clark's SL units A to M were also identified, and the lithostratigraphic succession was even expanded by three underlying lithostratigraphic units A1, A2, and A3 as demonstrated in CESAR core 83-14 (JACKSON et al. 1985, MUDIE & BLASCO 1985, for discussion see CLARK et al. 1990).

To obtain a chronological framework, the lithostratigraphic units were correlated to paleomagnetic records determined in these cores. This first chronology of sediment cores from the Amerasian Basin was based on the assumption that zones with negative inclination represented genuine polarity reversals (STEUERWALD et al. 1968, CLARK 1970, CLARK et al. 1980, MINICUCCI & CLARK 1983). At that time, geomagnetic excursions had not been considered as an alternative to polarity reversals when interpreting paleomagnetic data in sediment cores (see below). Thus, the first encountered down-core zone with negative inclination occurring within SL unit K (Fig. 4), was interpreted to represent the Brunhes/Matuyama boundary. Later, the original age model was revised several times (JONES 1987, DARBY et al. 1989, CLARK et al. 1990, CLARK 1996; for details see BACKMAN et al. 2004). The situation becomes even more complicated when considering that the magnetic reversals may also be interpreted in terms of geomagnetic excursions, as already mentioned by DARBY et al. (1989) in their synthesis paper.

As shown in several studies during the last decade, many measured changes in Pleistocene magnetic polarity directions in Arctic Ocean sediments probably represent geomagnetic excursions of shorter durations within the Brunhes Chron rather than full geomagnetic reversals (e.g., JAKOBSSON et al. 2001, NOWACZYK et al. 2001, 2003, BACKMAN et al. 2004, SPIELHAGEN et al. 2004). For the Lomonosov Ridge area, a detailed late Pleistocene stratigraphy has been developed at core 96/12-1pc (for location see Fig. 2) using sediment physical properties including colour, paleomagnetism, biostratigraphy, chemostratigraphy, and optically stimulated luminescence (OSL) dating (JAKOBSSON et al. 2000, 2001, 2003). In this revised chronostratigraphy, which is now widely accepted (e.g., BACKMAN et al. 2004, POLYAK et al. 2004, SPIELHAGEN et al. 2004, STEIN 2008 for review and further references), the Brunhes-Matuyama boundary is replaced with the Biwa II excursion (~220 ka, LUND et al. 2006). In the review by STEIN (2008), instead of the Biwa II excursion the Pringle Falls excursion (~240 ka, LUND et al. 2006, THOMPSON & GOLDSTEIN 2006) is proposed (Fig. 4). In any case, this polarity change determined in SL Unit K probably occurred within MIS 7, and it implies that sedimentation rates are about a factor of 3 to 4 higher than previous estimates. Very recently, ADLER et al. (2009) proposed that the changes in inclination determined in HOTRAX-2005 cores from Mendeleev Ridge are lithologically rather than geomagnetically controlled, and
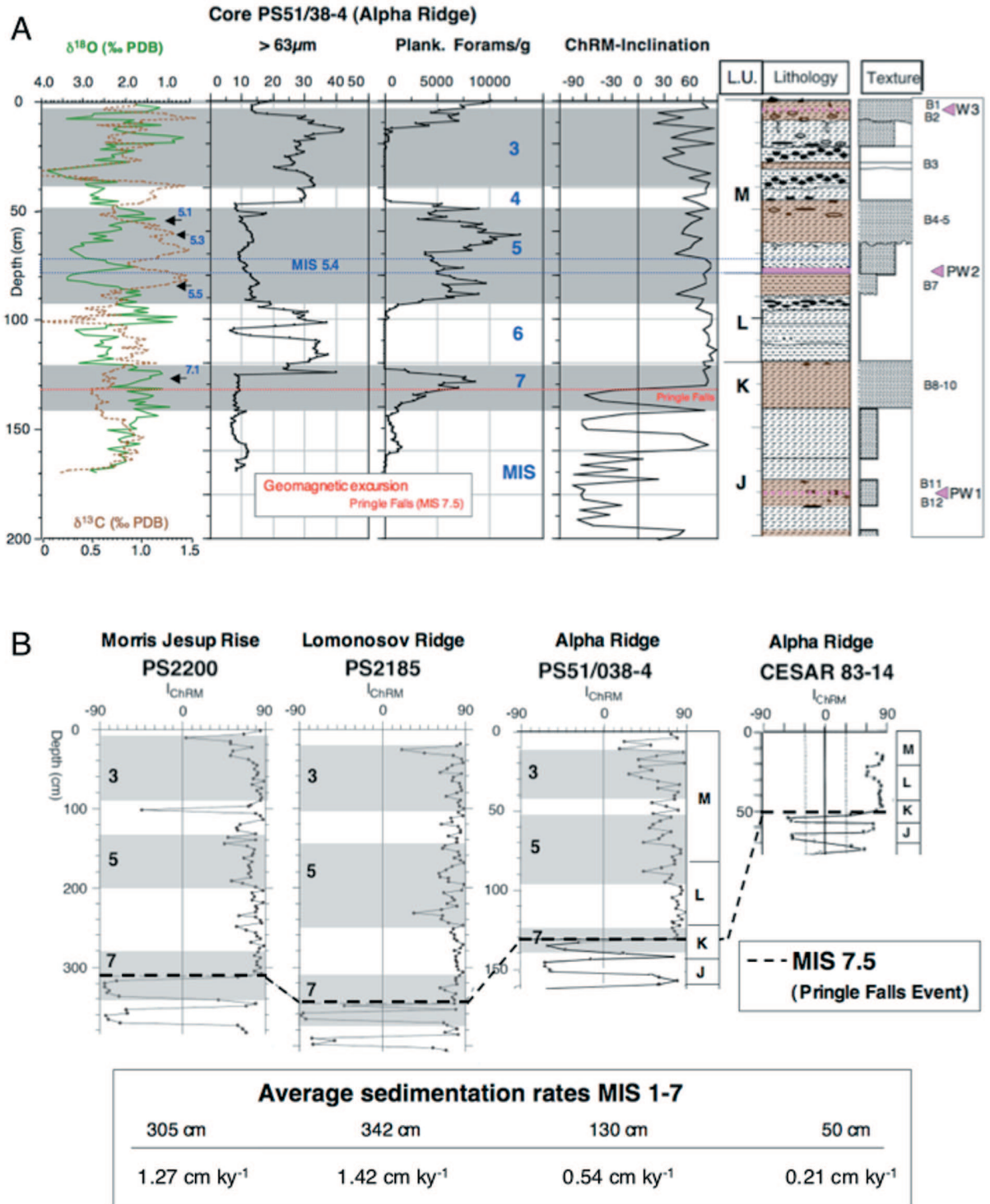
Fig. 4: (A) Records of stable oxygen and carbon isotopes of planktic foraminifer *Neogloboquadrina pachyderma* sin., coarse fraction >63 μm, abundance of planktic foraminifers and ChRM inclination of the upper 200 cm of core PS51/38-4 (for location of core see Fig. 3) (from SPIELHAGEN et al. 2004, supplemented). The magnetic polarity change at 132 cm core depth is related to the Pringle Falls Event (STEIN 2008). In addition, the main lithologies of standard lithostratigraphic (SL) units J to M and depths of pink layers are shown (from Stein et al. 1999). The PW2 layer coincides with prominent minima in the δ18O and δ13C records, interpreted as meltwater and IRD discharge during MIS 5d (STEIN 2008).
(B) Correlation and re-interpretion of the upper part of ChRM inclination (I_ChRM) records of cores PS2200, PS2185, and PS51/038-4 (SPIELHAGEN et al. 2004), and CESAR 83-14 (AKSU 1985), representing the time interval MIS 7 to MIS 1, and correlation with SL units J to M of CLARK et al. (1980). In addition, mean sedimentation rates for the time interval MIS 7 to MIS 1 are shown (from STEIN 2008).

Abb. 4: (A) Verteilung der stabilen Sauerstoff- und Kohlenstoffisotope der planktischen Foraminifere *Neogloboquadrina pachyderma* sin., der Grobfraktion >63 μm, der Häufigkeit der planktischen Foraminiferen und ChRM-Inklination der oberen 200 cm im Kern PS51/38-4 vom Alpha-Rücken (Lokation siehe Abb. 3, ergänzt nach SPIELHAGEN et al. 2004). Der magnetische Polaritätswechsel bei 132 cm Kerntiefe wird mit dem *Pringle Falls Event* korreliert (STEIN 2008). Zusätzlich sind die Hauptlithologien der lithostratigraphischen Standard (SL)-Einheiten J bis M (nach CLARK et al. 1980) und die Tiefen der „pink-white layers" dargestellt (nach STEIN et al. 1999, STEIN 2008).
(B) Korrelation und Neu-Interpretion des oberen Teils der ChRM-Inklination (I_ChRM)-Kurven der Kerne PS2200, PS2185 und PS51/038-4 (SPIELHAGEN et al. 2004), und des Kerns CESAR 83-14 (AKSU 1985) und Korrelation mit SL-Einheiten J bis M von CLARK et al. (1980). Zusätzlich sind die mittleren Sedimentationsraten für das Zeitintervall MIS 7 bis MIS 1 angeführt (aus STEIN 2008).

may coincide with changes in concentration of authigenic iron oxides (CHANNELL & XUAN 2009). Thus, these authors refrain from using inclination for correlation with global geomagnetic events, although some of the inclination changes might represent real variations in the geomagnetic field.

In sediment cores from the central Arctic Ocean, distinct (cyclic) alternations of (dark) brown and beige to gray lithological units are described (Fig. 5; e.g., JAKOBSSON et al. 2000, PHILLIPS & GRANTZ 2001, POLYAK et al. 2004, NØRGAARD-PEDERSEN et al. 2007a, 2007b).

The brown beds, probably representing interglacial/interstadial periods including the surficial Holocene interval, generally contain low to moderate amounts of IRD, faunal remnants, and manganese (Mn) oxides, whereas the beige to gray beds, corresponding to glacial/deglacial periods, are almost unfossiliferous and largely fine-grained, but may contain prominent IRD layers near the top and/or bottom of gray units that often extend into the adjacent brown interglacial unit (PHILLIPS & GRANTZ 2001, DARBY et al. 2006). According to their age model, which is based on paleomagnetism, nannofossil biostratigraphy, and cyclic variability in colour and Mn content, JAKOBSSON et al. (2000) proposed that the Mn and

colour variability follows low-latitude oxygen isotope oscillations. This Mn- and colour-derived time scale is independently supported by the paleomagnetic record, control points of nannofossil occurrences, and OSL datings (JAKOBSSON et al. 2000, 2001, 2003). The Mn cycles may reflect changes in riverine Mn input and/or variation in the degree of sediment oxidation resulting from changes in ventilation of bottom waters, although the exact mechanisms for these changes are still speculative (JAKOBSSON et al. 2000, POLYAK et al. 2004).

In summary, it can be stated that (i) in general sediment cores from the Amerasian Basin and the Eurasian Basin can be correlated quite well based on micropaleontological proxies, paleomagnetic proxies, and [10]Be records, (ii) a generally consistent age model for the time interval down to MIS 7 can be obtained (BACKMAN et al. 2004, 2009, SPIELHAGEN et al. 2004) although – especially for the Amerasian Basin – some discrepancies still occur when looking at details (see Fig. 5, different age models proposed by DARBY et al. 2006, ADLER et al. 2009, BACKMAN et al. 2009, POLYAK et al. 2009), and (iii) below MIS 7 additional independent age proxies are certainly needed to improve the chronology.
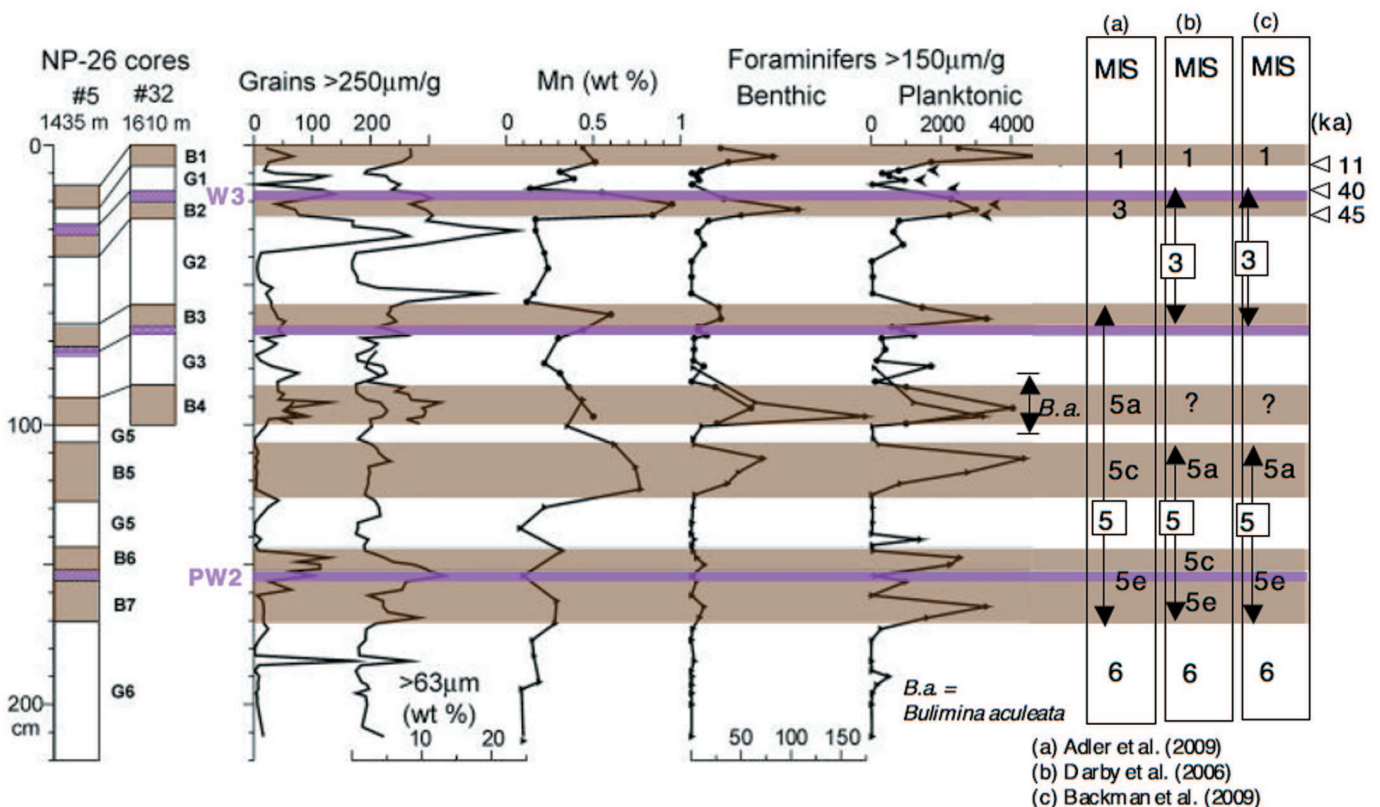

Fig. 5: Stratigraphy, amount of coarse fraction >250 µm and >63µm, manganese content, and abundances of planktic and benthic foraminifers of bottom sediments from cores NP-26-5 and NP-26-32 (combined as NP-26 record) from the Mendeleev Ridge, western Arctic Ocean (from POLYAK et al. 2004, supplemented). Index numbers to the right of lithologic columns show lithologic units (B1-B7 = brown intervals, G1-G6 = gray intervals). Brown (interglacial) intervals are marked as brown bars, pink bars indicate pink-white detrital-carbonate layers used as stratigraphic markers. MIS stratigraphy of the interglacials proposed by (a) ADLER et al. (2009), (b) DARBY et al. (2006), and (c) BACKMAN et al. (2009) are shown at the right-hand side. The latter is based on nannofossil stratigraphy from Core HLY0503-8JPC and correlation to Core NP-26. For location of cores see Figure 3. Ages of 11, 40, and 45 ka are average AMS14C datings in calendar kilo-years BP (POLYAK et al. 2004, 2009).

Abb. 5: Stratigraphie, Anteil der Grobfraktionen >250 µm und >63 µm, Mangan-Gehalt und Häufigkeit der planktischen und benthischen Foraminiferen der Kerne NP-26-5 und NP-26-32 vom Mendeleev-Rücken, westlicher Arktischer Ozean (ergänzt nach POLYAK et al. 2004). Braune (interglaziale) Intervalle (B1 bis B7) sind als braune Balken gekennzeichnet. Isotopen-Stratigraphie der Interglaziale (rechte Seite) nach (a) ADLER et al. (2009), (b) DARBY et al. (2006), und (c) BACKMAN et al. (2009). Letztere basiert auf der Nannofossil-Stratigraphie von Kern HLY0503-8JPC und Korrelation zum Kern NP-26. Die Alter von 11, 40, und 45 ka sind mittlere AMS14C-Alter in tausend Kalender-Jahren BP vor heute (POLYAK et al. 2004, 2009).

MATERIAL AND METHODS

During "Polarstern" ARK-XXIII/3 expedition, a total of 15 geological stations with coring activities (Tab. 1) were carried out (JOKAT 2009, STEIN et al. 2009b). All coring positions were collected carefully using detailed multi-beam bathymetric mapping by Hydrosweep and sub-bottom PARASOUND aoustic profiling systems to avoid areas of sediment redeposition (turbidites and/or slumps) and erosion. At all stations shown on Figure 3 surface sediments were taken by giant box corer (GKG) and multicorer (MUC), and sediment cores were recovered either by gravity corer (SL) or a kastenlot (KAL) corer. Core PS72/392-5 is a re-coring at the site of Clark's key core FL-224 (for details see STEIN et al. 2010, this vol.).

Before opening, all sediment cores were logged for physical properties (magnetic susceptibility, density, and p-wave velocity) using the Multi Sensor Core Logger (MSCL, GEOTEK Ltd., UK; WEBER et al. 1997, ROTHWELL 2006).

After opening, from the archive half of all core sections photographs were taken, and a detailed visual core description was carried out. Colour of sediments was described using the Munsell Soil Colour Chart. For main lithologies, smear-slide analyses were performed for rough evaluation of grain-size composition, preliminary determination of mineralogical composition (quartz, feldspars, carbonates, opaques), and content of biogenic components (foraminifers, coccoliths, diatoms, sponge spicules).

Spectral reflectance was measured on freshly split core surfaces that were covered with transparent wrap with a hand held spectrophotometer (Minolta CM 2002, lens diameter 8 mm, field of view Ø 0.8 cm) at wave lengths from 400 to 700 nm (10 nm steps), connected to a MACINTOSH Powerbook 5300C. Output files are the L*a*b* colour space that is also referred to as CIELAB space (Commission Internationale de l'Éclairage L*a*b colour space 1976), the chroma, hue and value of the Munsell Colour Chart, the percentage value of the spectrum at 10 nm steps from 400 to 700 nm, and the colour values x, y and z that are defined according to the RGB colours. Lightness L* (grey scale) is recorded from 0 % (black) to 100 % (white), the red-green colour space a* from green to red, and the yellow-blue colour space b* from blue to yellow (SCHRECK et al. 2009 for some more details). The lightness (L*) values presented in this paper, are uncorrected raw data.

Undrained shear strength was measured with a hand held shear vane, equipped with a 19 mm blade (Geotechnics, Auckland, New Zealand). The measurements were conducted on selected kastenlot and gravity cores (PS72/287-3, PS72/340-5, PS72/342-1, PS72/343-1, PS72/344-3 and PS72/350-2; for locations see Fig. 3) at irregular intervals in the center of the split cores.

X-Ray photographs were taken from sediment slabs (25 x 10 x 0.8 cm each) in order to count the numbers of coarse grains >2 mm (mainly related to IRD, GROBE 1987) and to study the sediment structures in detail (MATTHIESSEN et al. 2010, this vol.). The IRD >2 mm data presented this paper, are uncorrected raw data.

For coarse-fraction analysis, the fraction >63 μm was isolated by means of wet sieving; the sand fraction was further split into subfractions. In order to roughly estimate the abundance of the major sediment components (siliciclastics, detrital carbonates, planktic and benthic foraminifers, ostracods, etc.), the fractions between 125 and 500 μm was analysed using a binocular microscope. The abundance of each component was simply expressed in six categories: absent, traces/very rare, rare, common, abundant, and dominant (NAM 2009).

RESULTS

Mendeleev Ridge – southern sampling transect (77°40' N)

Five sediment cores (PS72/340-5, PS72/341-5, PS72/342-1, PS72/343-2, and PS72/344-3) were recovered along a transect from the Chukchi Abyssal Plain across the southern Mendeleev Ridge toward the East Siberian continental margin (Fig. 3). The sediments of these cores are characterized by prominent changes in sediment colour, grain-size, sediment composition, and degree of bioturbation (Fig. 6). In all the cores, prominent dark brown intervals were found, which together with the pink-white layers and microfossil abundance are used for core correlation and age control.
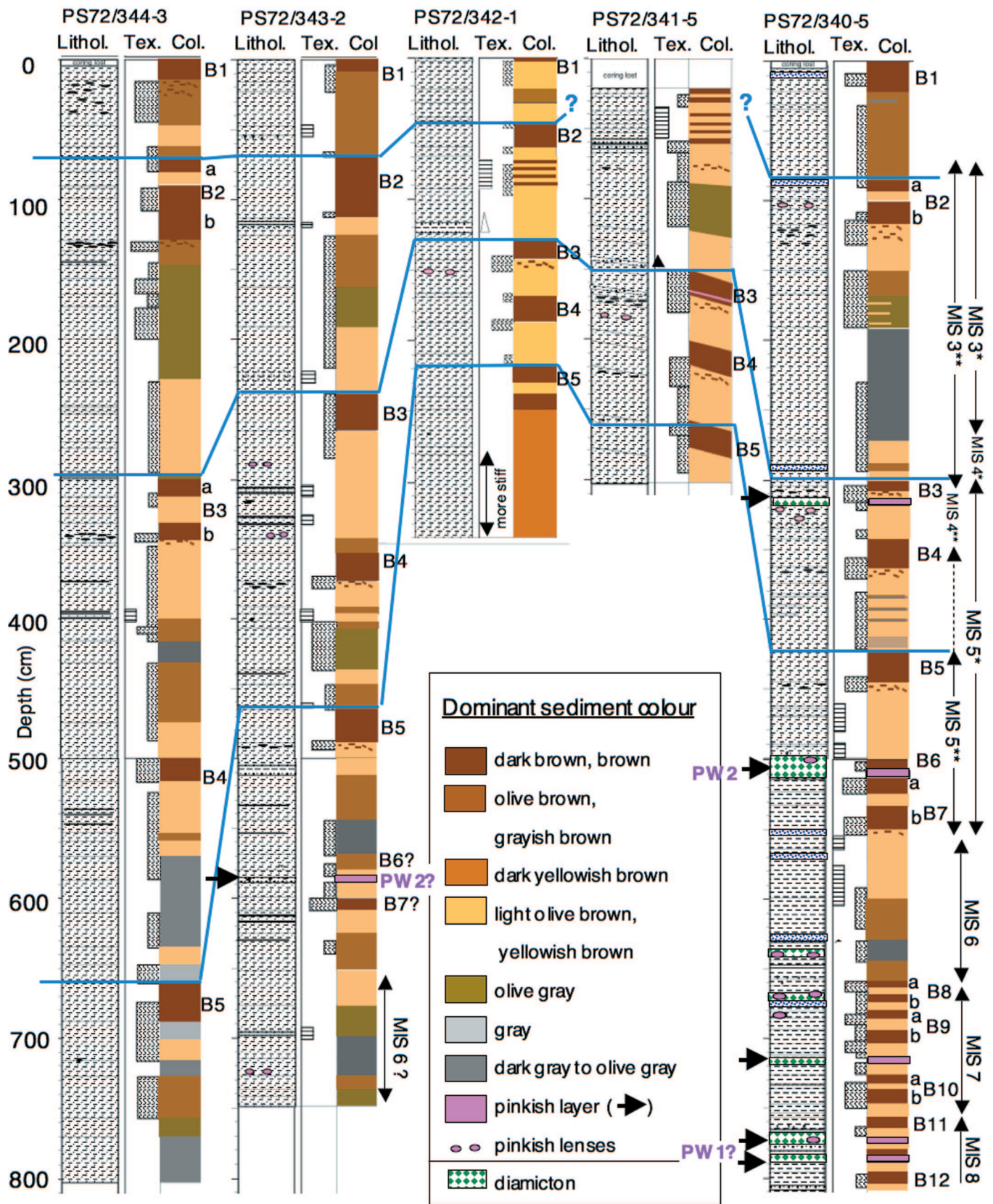
Station	Gear	Latitude	Longitude	Water depth (m)
PS72/340-5	KAL	77°36.31'N	171°29.09'W	2349
PS72/341-5	KAL	77°36.11'N	176°06.23'W	1368
PS72/342-1	GC	77°36.01'N	177°20.62'W	819.8
PS72/343-2	GC	77°18.33'N	179°02.73'W	1225
PS72/344-3	KAL	77°36.62'N	174°32.37'W	1257
PS72/392-5	GC	80°27.81'N	158°49.75'W	3624
PS72/392-6	GKG	80°28.42'N	158°50.83'W	3637
PS72/396-3	GKG	80°35.17'N	162°22.57'W	2733
PS72/396-5	KAL	80°34.74'N	162°10.01'W	2722
PS72/399-3	GKG	80°38.48'N	166°42.99'W	3375
PS72/399-4	GC	80°39.18'N	166°45.81'W	3376
PS72/404-3	GKG	80°45.39'N	171°09.69'W	2182
PS72/404-4	GC	80°45.29'N	171°09.63'W	2181
PS72/408-3	GKG	80°32.92'N	174°40.17'W	2576
PS72/408-5	GC	80°33.11'N	174°41.77'W	2583
PS72/410-1	GKG	80°30.37'N	175°44.38'W	1802
PS72/410-3	KAL	80°31.29	175°43.49'W	1847
PS72/413-3	GKG	80°16.49'N	178°31.29'W	1261
PS72/413-5	GC	80°17.25'N	178°29.27'W	1273
PS72/418-5	GKG	80°23.54'N	178°49.00'E	2045
PS72/418-7	GC	80°23.93'N	178°51.34'E	2043
PS72/422-3	GKG	80°33.08'N	175°44.75'E	2547
PS72/422-5	KAL	80°32.68'N	175°44.63'E	2536
PS72/430/4	GC	81°03.38'N	164°43.72'E	2874

Tab. 1: Locations and water depths of geological stations carried-out during „Polarstern" ARK-XXIII/3 expedition in 2008 and discussed in this paper (for complete list of all geological stations see JOKAT 2009).

Tab. 1: Lokationen und Wassertiefen ausgewählter geologischer Stationen der „Polarstern"-Expedition ARK-XXIII/3 (JOKAT 2009).
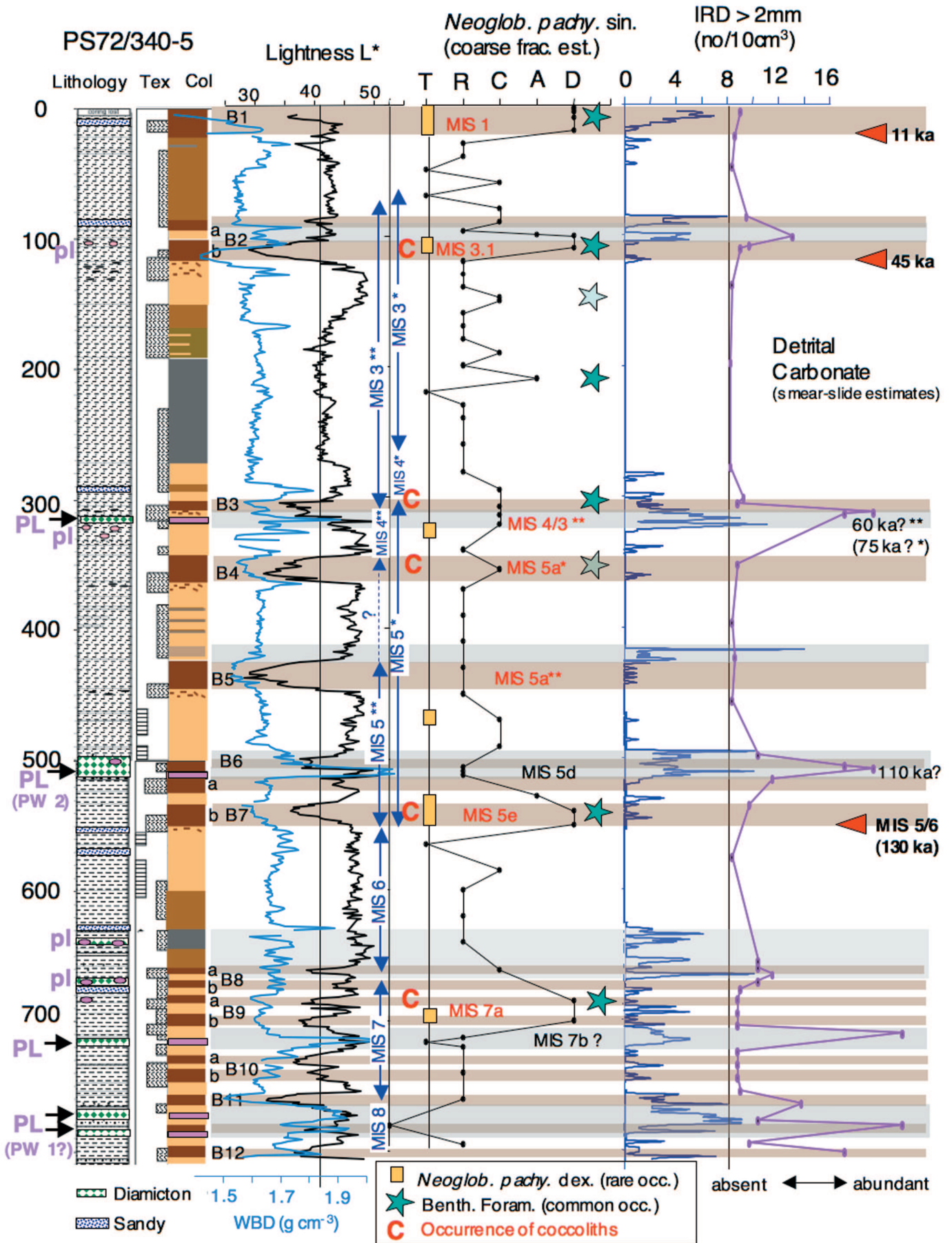
Fig. 6: Simplified summary of lithologies and main sediment colours in sediment cores PS72/340-5, PS72/341-5, PS72/342-1, PS72/343-2, and PS72/344-3 across the southern Mendeleev Ridge. Main brown to dark brown intervals (B1 to B5) and pink-white (PW) layers were used for correlation and to obtain a preliminary age model; (*) = age model proposed by ADLER et al. (2009) and POLYAK et al. (2009), (**) = age model based on nannofossil stratigraphy from Core HLY0503-8JPC (BACKMAN et al. 2009) and correlation to Core NP-26 (see also Fig. 7).

Abb. 6: Vereinfachte Darstellung der Lithologie und Sedimentfarbe in den Kernen PS72/340-5, PS72/341-5, PS72/342-1, PS72/343-2 und PS72/344-3 über den südlichen Mendeleev-Rücken (vgl. Abb. 3). Zur Stratigraphie siehe Abb. 7.

Main lithologies

Looking at the lithology of core PS72/340-5 in more detail, different types of sediment facies can be distinguished (Fig. 7): Alternations of dark grayish brown, dark brown and brown silty clay and light olive brown silty clay, with variable degree of bioturbation, are the predominent lithologies from 0 to 167 cm and 272 cm to the bottom of the section. In between (167 to 272 cm core depth), olive gray to dark gray silty clay is typical. Between 380 and 420 cm and, especially, between 630 and 644 cm also dark gray colours occur. The dark brown intervals are characterized by prominent minima in the lightness L* and – in most cases – also the wet bulk density. Furthermore, several of the dark brown intervals display increased abundances of planktic and benthic foraminifers and coccoliths. These horizons are useful tools for core correlation and stratigraphy (see discussion).

At 314-316 cm and at 498-513 cm, 714-718 cm, and 785-787 cm, prominent horizons of very pale brown („white“) and light reddish brown („pinkish“), respectively, sandy silty clay intervals with several dropstones (diamictons) and increased amount of detrital carbonate were found in the PS72/340-5 sequence (Fig. 7). In the horizon at 498-513 cm, dropstones (dolomite) may reach a size of up to 10 cm in diameter (Fig. 8). Between about 540 and 680 cm, horizons with elevated sand content are more typical (Fig. 7). According to CLARK et al. (1980), these „pinkish“ (white or pink-white) horizons are important lithostratigraphic marker horizons (see discussion). In addition to the prominent pinkish layers, small pinkish
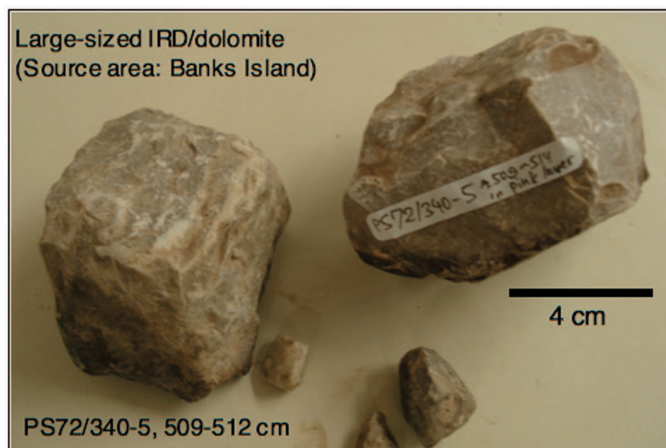

Fig. 8: Large-sized dropstones (dolomite) from the pink-white layer PW2 (498-513 cmbsf) in Core PS72/340-5 (cf., Fig. 7).

Abb. 8: Großes Eis transportiertes Dolomit-Geröll (dropstone) aus der "pink-white layer" PW 2 (498-513 cmbsf) in Kern PS72/340-5 (vgl. Fig.7).

lenses were found at 102-103 cm, 321-326 cm, 637-639 cm, 670-671 cm, 680-686 cm, 771-772 cm, and 775-776 cm. Thus, it is obvious that more than the three pink-white layers described by CLARK et al. (1980), may occur in cores with high sedimentation rates (see also ADLER et al. 2009). This is important to know when using the pink-white layers for core correlation.

Mendeleev Ridge – northern sampling transect

On a 700 km long transect along about 80°30' N from the Canada Basin across the central Mendeleev Ridge into the Makarov Basin 12 sediment cores were retrieved (see Fig. 3 for locations). Except for core PS72/393-4 representing a 550 cm thick sequence dominated by grayish distal turbidite layers (STEIN et al. 2009b), the predominent lithologies of all sediment cores are silty clay or clayey silt („mud“) of brown to dark brown, light to dark yellowish brown, and light olive brown colours (Figs. 9 and 10). In the upper about 2.5-4 m of most of the cores, more sandy intervals (sandy silty clay), dropstones, and mud clasts occur.

Main lithologies

In cores PS72/418-7 and PS72/422-5 located on the Makarov Basin side of Mendeleev Ridge, more sandy intervals occasionally also occur in the lower part of the sequences. Also in the northern transect, the most prominent features of all cores are colour cycles of brown to dark brown and light olive brown to yellowish brown (beige) sediments occurring down to the bottom of the cores. Most of the sediments are slightly to strongly bioturbated. Furthermore, specific marker horizons (i.e., pink-white and white layers; see above) could be identified in all these cores. In general, the sedimentary sequences can be divided into two main units. Unit I is composed of alternations of silty clays and more sandy intervals, partly with mud clasts and dropstones, whereas Unit II is mainly composed of fine-grained sediments (silty clays) with brown/light olive brown colour cycles (Fig. 10).

Similar to the records of core PS72/340-5 (Fig.7), the colour changes and cyclicities are also reflected in the lightness records, as shown for cores PS72/392-5, PS72/396-5, PS72/399-4, and PS72/404-4 (Fig. 11). In general, the dark-brown to brown intervals correlate with low lightness values whereas the dominantly light olive-brown as well as the lighter sandy intervals correlate with high lightness values. The most prominent pink-white layers coincide with high lightness values (Fig. 11). In the lower part of all the four records, dark

Fig. 7: Core PS72/340-5 from eastern Mendeleev Ridge. Simplified summary of lithologies, main sediment colours, wet bulk density (WBD = blue curve), lightness L* = black curve), estimates of abundances of *N. pachyderma* sin. (T = traces/very rare, R = rare, C = common, A = abundant, D = dominant), IRD grains >2 mm = blue curve, relative abundance of detrital carbonate determined by smear-slide analysis (red curve). C = occurrence of coccoliths based on smear-slide analysis, blue stars = common occurrence of benthic foraminifers, yellow squares = rare occurrence of *N. pachyderma* dex. estimated from coarse fraction 250-500 μm. PL = pink-white layers, pl = pink-white lenses. PW 1 and pw 2 indicate pink-white layers according to CLARK et al. (1980). Proposed MIS stages/substages of upper part (B1 to B7) based on POLYAK et al. (2004, 2009), * = stratigraphy based on ADLER et al. (2009), ** = based on BACKMAN et al. (2009), MIS 5d proposed by STEIN (2008), see also Figures 4 and 5.

Abb. 7: Kern PS72/340-5 vom östlichen Mendeleev-Rücken: Vereinfachte Darstellung der Lithologien und Sedimentfarben, derNassdichte (WBD = blau), Helligkeit = L*, Häufigkeit von N. pachyderma sin. (T = sehr selten, R = selten, C = gewöhnlich, A = häufig, D = dominant), Anzahl der Eis transportierten Körner >2 mm (IRD = blaue Kurve), relative Häufigkeit von detritischem Karbonat nach Smear-slide-Analysen (rote Kurve). C (rot) = Vorkommen von Coccolithen, Sterne (blau) = Vorkommen benthischer Foraminiferen, Rechtecke (gelb) = Vorkommen von N. pachyderma dex. abgeschätzt aus der Grobfraktion 250-500 μm. PW 1 und pw 2 stehen für die "pink-white layers" nach CLARK et al. (1980). Isotopenstadien (MIS) des oberen Kernabschnitts (B1 bis B7) nach POLYAK et al. (2004, 2009), * = nach ADLER et al. (2009), ** = nach BACKMAN et al. (2009), MIS 5d nach STEIN (2008); siehe auch Abbildungen 4 und 5.
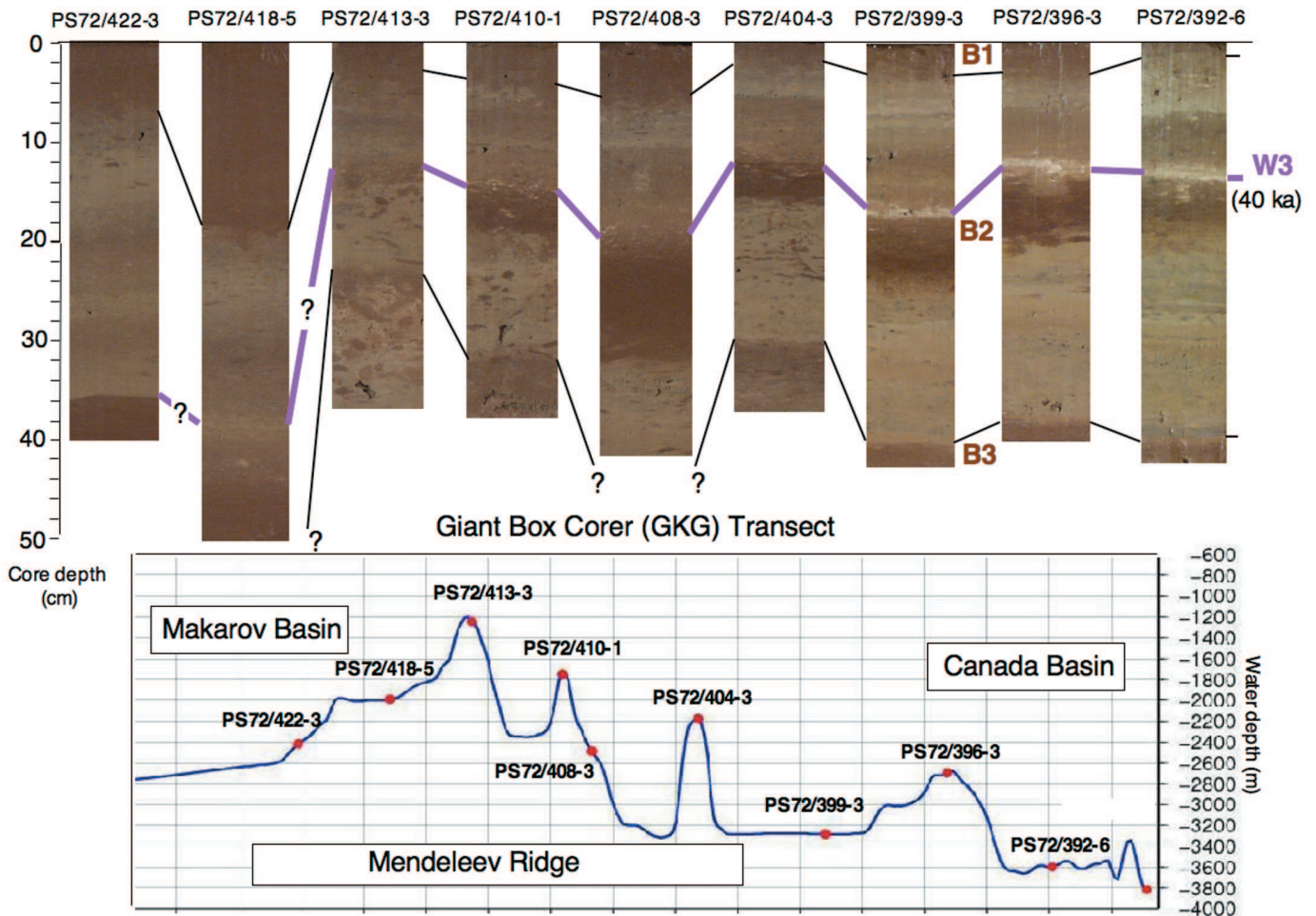
Fig. 9: Photographs of giant box corer (GKG) cores recovered along the northern transect across Mendeleev Ridge (for core location see Fig. 3 and Tab. 1). Dark brown intervals B1, B2 and B3, white layer W3, and correlation lines are indicated. Age of W3 based on POLYAK et al. (2004, 2009).

Abb. 9: Fotos der Kerne aus Großkastengreifern (GKG) vom nördlichen Transekt über den Mendeleev-Rücken (Kern-Lokationen siehe Abb. 3 und Tab. 1). Die dunkelbraunen Intervalle B1, B2, B3, und die "white layer" W3 sowie Korrelationslinien sind angezeigt. Alter für W3 nach POLYAK et al. 2004, 2009).

brown and dark reddish brown colours become more predominant (for see detailes STEIN et al. 2009b), indicated by a prominent drop in the lightness records (Fig. 11).

For cores PS72/396-5 and PS72/410-3, data on the composition of coarse fraction are available (NAM 2009). Terrigenous grains are dominated by quartz and relatively high amounts of feldspar and ("golden-coloured") mica with minor amounts of rock fragments, carbonate, heavy minerals and basalt. Similar to the cores from the southern transect, monospecific planktic foraminifer assemblages of *N. pachyderma* sin. form the most dominant biogenic component while calcareous benthic foraminifera are rare to common. At core PS72/396-5, calcareous planktic and benthic foraminifers are restricted to the upper 2 m, while rare agglutinated benthic foraminifers occurred below 4 m core depth (NAM 2009): a similar distribution pattern of foraminifers was found at core PS72/410-3. At core PS72/392-5 this change is contemporaneous with the occurrence of biogenic calcite (determined by LECO and XRD analyses) and calcareous foraminifers (determined in smear slides) (STEIN et al. this vol.), both supporting the stratigraphic correlation based on lithologies (Fig. 10).

DISCUSSION

Lithostratigraphy, age model and sedimentation rates across Mendeleev Ridge

Although major progress has been made during the last years concerning Quaternary stratigraphy of the central Arctic Ocean sediments (JAKOBSSON et al. 2001, BACKMAN et al. 2004, 2009, POLYAK et al. 2004, 2009, SPIELHAGEN et al. 2004, O'REGAN et al. 2008), a definitive judgement regarding an age model for these sediments has still to be done with caution. Because age model choice strongly affects the interpretation of paleoceanographic evolution, this uncertainty prompts an urgency in refining and verifying the chronostratigraphy for the Arctic Ocean sediments (POLYAK et al. 2004). In this context, past, ongoing and future studies of the new high-quality sediment cores recovered in the Amerasian Basin during the "Polarstern" ARK-XXIII/3 expedition in 2008 (JOKAT 2009) as well as the HOTRAX Expedition in 2005 (DARBY et al. 2005, ADLER et al. 2009, BACKMAN et al. 2009, POLYAK et al. 2009) may help to solve this problem. Here, a preliminary stratigraphy and a tentative age model for the ARK-XXIII/3 sediment cores based on shipboard lithological and micropaleontological data and correlation with other
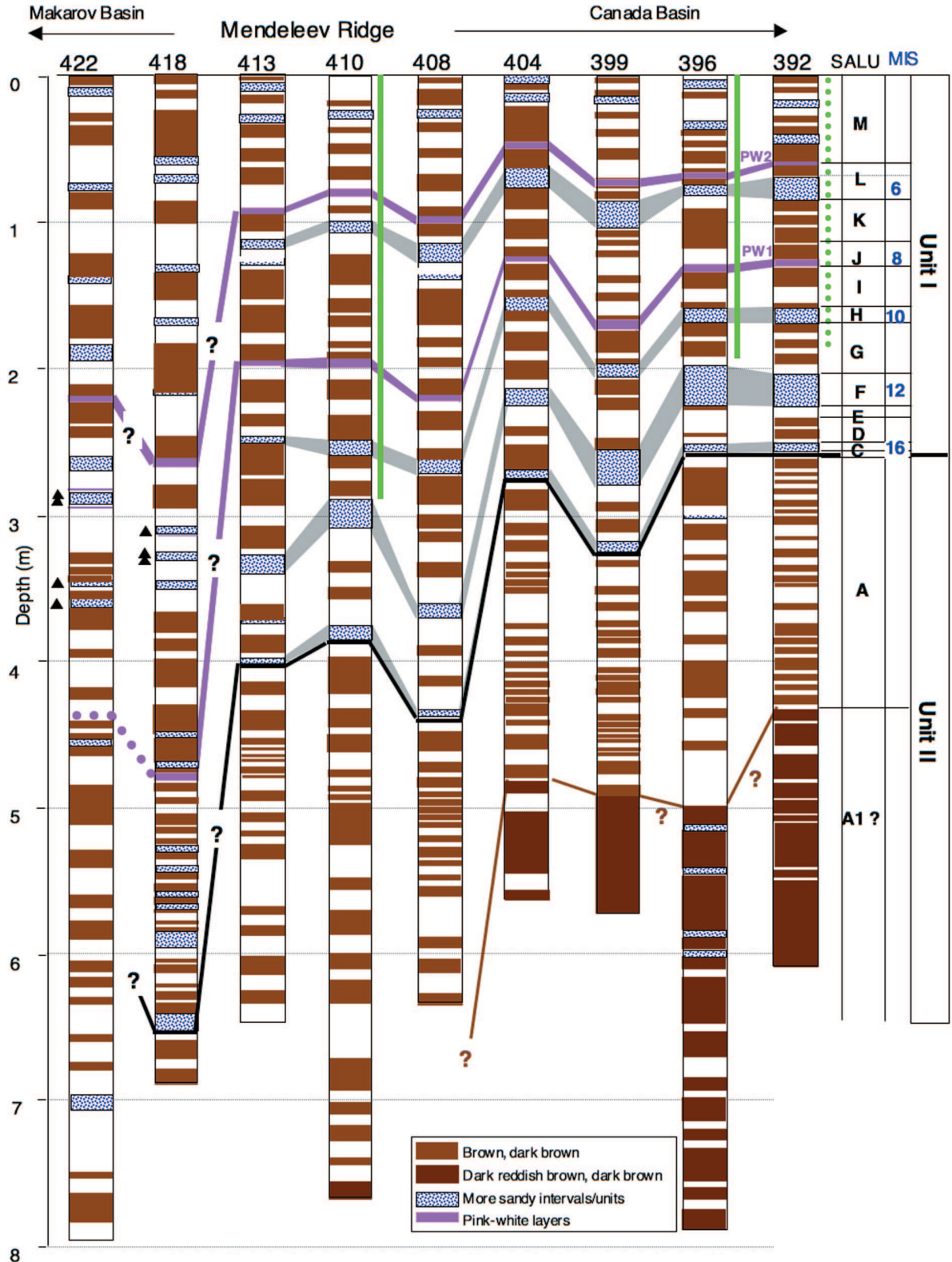
Fig. 10: Simplified scheme of the occurrence of brown, dark brown, and dark reddish brown layers, more sandy intervals/units, and main pink-white layers in sediment cores from the northern transect across Mendeleev Ridge (for core locations see Fig. 3). Vertical green bars at records of cores PS72/396-5 and PS72/410-3 mark occurrence of planktic foraminifers (dominantly *N. pachyderma* sin.) as determined in the coarse fraction (NAM 2009), vertically stippled line at record of core PS72/392-5 marks occurrence of (biogenic) calcite (based on XRD analysis) and foraminifers in smear slides (STEIN et al. this vol.). Standard lithostratigraphic (SL) units A1 to M (according to CLARK et al. 1980), main lithological units I and II, and depths of main pink-white layers PW1 and PW2 are indicated. Based on our preliminary age model, the sandy SL units L, J, H, F, and C may fall into MIS 6, 8, 10, 12, and 16, respectively.

Abb. 10: Vereinfachtes Schema der Vorkommen der (dunkel-) braunen Intervalle und der sandigen Abschnitte, die in die lithostratigraphischen Standard (SL)-Einheiten L, J, H, F, und C fallen und neben den "pink-white layers" PW1 und PW2, die Grundlage für die Korrelation der Kerne sind. Die SL-Einheiten A bis M (nach CLARK et al. 1980), die lithologischen Grundeinheiten (Unit I, Unit II) sowie Marine Isotopenstadien (MIS) 6, 8, 10, 12 und 16 sind am rechten Abbildungsrand angegeben. Die grünen Balken in den Kernen PS72/396-5 und PS72/ 410-3 markieren Vorkommen planktischer Foraminiferen (hauptsächlich *N. pachyderma* sin., NAM 2009). Die grünen Punkte in Kern PS72/392-5 markieren das Vorkommen von (biogenem) Kalzit (STEIN et al. dieses Heft).
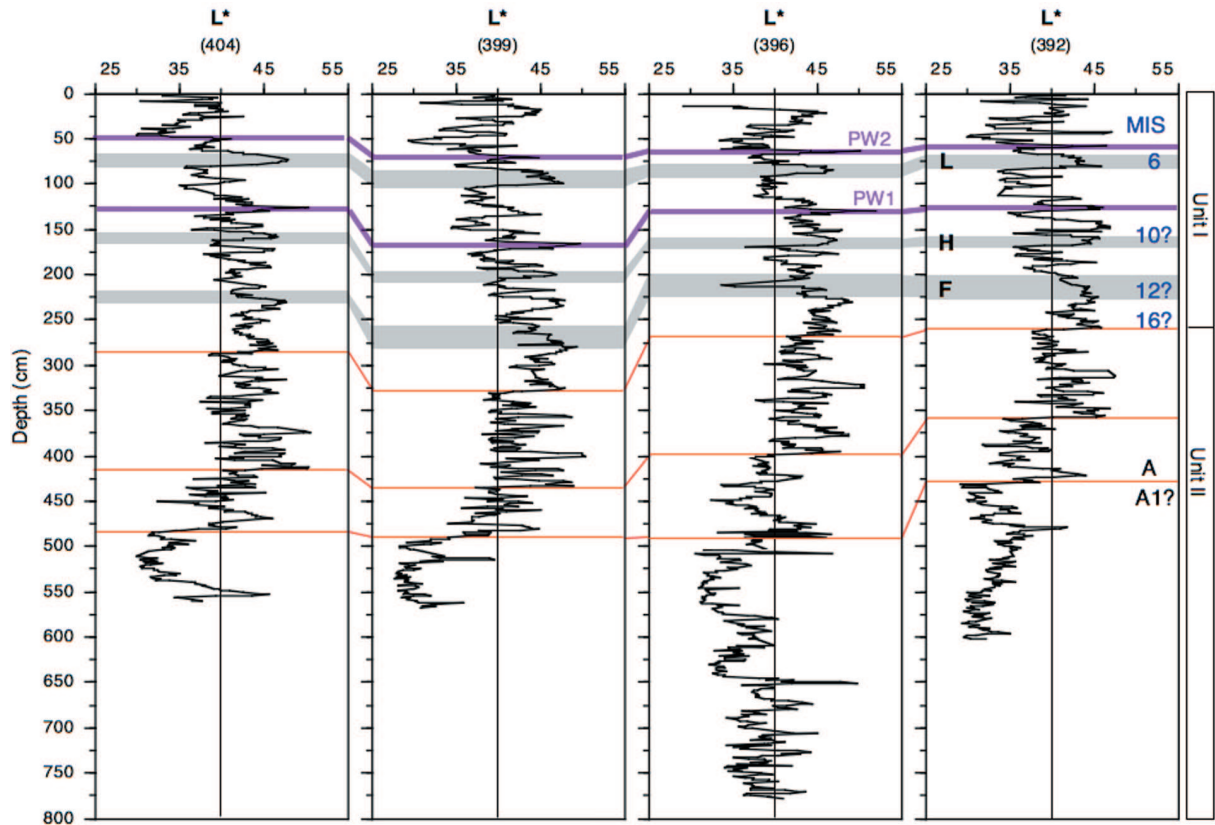
Fig. 11: Correlation of sediment cores by Lightness (L*) records of cores PS72/392-5, PS72/396-5, PS72/399-4, and PS72/404-4 (for core locations see Fig. 3). Gray bars = major sandy intervals/SL units L, H, and F; PW1 and PW2 = main pink-white layers; some further correlation lines (in red), and proposed Marine Isotope Stages (MIS) are indicated.

Abb. 11: Helligkeitskurven (L*) der Kerne PS72/392-5, PS72/396-5, PS72/399-4 und PS72/404-4. Graue Balken = Sand-Intervalle/SL-Einheiten L, H, and F, PW1 und PW2 = "pink-white layers", einige Korrelationslinien (in rot) und vorgeschlagene Marine Isotopenstadien (MIS) sind angezeigt.

dated sediment cores, are presented. An alternative (very different) age model mainly based on the assumption that there is a synchronous onset of circum-Arctic diamicton deposition, is discussed by MATTHIESSEN et al. (2010, this vol.).

Based on the visual core description, the standard lithological (SL) units A to M developed by CLARK et al. (1980), could also be clearly identified in the ARK-XXIII/3 sediment cores from our northern transect across Mendeleev Ridge (Fig. 10; Tab. 2). Following CLARK et al. (1980), the content of sand-sized material (enriched in SL units C, F, H, J, L, and parts of M) and the pink-white layers were considered to be the key sedimentary characteristics used for correlation of these SL units. In our cores, this lithostratigraphic correlation is supported by the (dominant) occurrence of planktic foraminifers in the coarse fraction of samples from SL units M to G (cores PS72/392-5, PS72/396-5, and core PS72/410-3). In some cores (e.g., PS72/392-5, PS72/396-5, PS72/399-4, and PS72/ 404-4), a lithostratigraphic unit underlying SL unit A (unit A1 according to MUDIE & BLASCO 1985) was probably also recovered (Fig. 10). In addition, the dark brown horizons (cf., JAKOBSSON et al. 2000, POLYAK et al. 2004) are key elements for our tentative stratigraphic framework.

Using the upper seven, prominent dark brown intervals (B1 to B7), it seems to be possible to correlate the cores along the southern as well as northern transects across Mendeleev Ridge

(Figs. 6, 10). For the giant box corer sections recovered along the northern transect and representing the uppermost 40 to 50 cm of the sequence (i.e., B1 to B3), this correlation is very prominent along the eastern ("Canadian") side of the Mendeleev Ridge and further supported by the correlation of the white layer W3 (Fig. 9). When using the dark brown intervals for core correlation of the deeper part of the sections, however, one should have in mind that the number of dark-brown intervals are not identical for all studied sediment cores. In some cores, a few thicker dark brown intervals occur, whereas in other cores several dark brown/beige alternations were found in the corresponding time intervals (Fig. 10). This may be explained on one hand by different sedimentation rates. On the other hand, different (diagenetic?) processes may have caused some of the dark brown layers (cf., MARTINEZ et al. 2009). If this is the case, core correlation based on the dark brown intervals should be used with caution and supported by other independent proxies. Further geochemical studies of different brown intervals may help to solve this problem.

In order to obtain a preliminary age model of the upper part of our cores, the upper seven brown intervals were related to corresponding brown intervals B1 to B7 at cores NP-26 and HLY0503-8JPC (POLYAK et al. 2004, 2009, DARBY et al. 2006, BACKMAN et al. 2009; see Fig. 3 for core locations). At these cores, the bases of brown intervals B1 and B2 are AMS[14]C-dated to 11,000 calendar years BP (11 ka) and about 45 ka,

Depth Interval (cm)	PS72/422	PS72/418	PS72/413	PS72/410	PS72/408	PS72/404	PS72/399	PS72/396	PS72/392	PS72/340
Layer W3 (SL or KAL) (W3 in GKG)	??	??	9-10	?? (17-17.5)	8-10 (19-23)	?? (11-13)	7-7.5 (17.5-18.5)	9-9.5 (12.5-15)	6.5-7.5 (13-14)	??
Layer PW2 (base MIS 5d)	220-221	260-266	83-92*	77-82	95-100	47-50	69-71*	63-66	57-59	507-513
SL unit L	221-328 (107)?	268-359 (91)?	92-129 (37)	82-105 (23)	100-126 (26)	50-75 (25)	71-101 (30)	66-88 (22)	59-83 (24)	513-658 (145)
upper brown part (~MIS 5e)	221-252 (31)?	268-301 (33)?	92-111 (19)	82-99 (17)	100-114 (14)	50-63 (13)	71-84 (13)	66-74 (8)	59-68 (9)	513-550 (37)
lower sandy part (~MIS 6)	252-328 (76)?	301-359 (58)?	111-129 (18)	99-105 (6)	114-126 12)	63-75 (12)	84-101 (17)	74-88 (14)	68-83 (15)	550-658 (108)
Layer PW1	430 **	475-479	195-196	192-202*	217-221*	123-128*	164-171*	128-133*	124-129*	771-787 ?
SL unit H	??	??	238-249 (11)	248-255 (7)	262-272 (10)	151-161 (10)	194-204 (10)	156-168 (12)	157-168 (11)	
(extrapolated age base Unit H in ka)			293	336	309	335	314	295	323	
SL unit F	??	??	325-338 (13)	286-309 (23)	351-369 (18)	215-226 (11)	250-276 (26)	194-225 (29)	202-224 (22)	
(extrapolated age base Unit F in ka)			398	407	419	471	425	395	431	
Depth Boundary Unit 1/2 (extrapolated age in ka)	??	648	398	382	437	274	320	261	255	
			468	503	497	571	492	458	490	

Tab. 2: Depth intervals of lithological marker horizons PW1, PW2, and W3, depth intervals and thicknesses of standard lithostratigraphic (SL) units L, H, and F (in brackets thickness), and depth of Unit I/Unit II boundary for sediment cores from the northern transect across the Mendeleev Ridge. For the W3 layer, depths from gravity/kastenlot cores and giant box cores are given. The latter (numbers in brackets) represent the undisturbed complete near-surface sediment sections whereas the former values are lower, probably related to loss and/or compaction in the sections recovered by gravity corer. For comparison, data from Core PS72/340-5 from the southern transect are listed as well. In addition, extrapolated ages of the base of SL units H, F, and C using mean MIS 1 to 5 sedimentation rates, are listed in red (see Tab. 3). * = in the PW layer, separate white (top) and pink (bottom) layers can be identidied; ** = dolomite-rich horizon interpreted as PW1 (SCHULTE-LOH 2009).

Tab. 2: Tiefenintervalle der lithostratigraphischen Leithorizonte PW1, PW1 und W3 und Mächtigkeiten der SL-Einheiten L, H, und F (in Klammern Mächtig-keiten) sowie Tiefe der Grenze zwischen den lithologischen Haupteinheiten I und II in Sedimentkernen vom nördlichen Transekt über den Mendeleev-Rücken. Für den Leithorizont W3 sind die Tiefenlagen im Schwerelot- (SL) bzw. Kastenlot-Kern (KAL) und auch im Großkastengreifer (GKG) dargestellt. Die GKG-Tiefen sind größer (Werte in Klammern), da sie eher die ungestörte Gesamtmächtigkeit der oberflächennahen Sedimente darstellen, während die niedrigeren Werte aus den SL- bzw. KAL-Kernen auf Sedimentverlust in den obersten cm oder auch Kompaktion zurückzuführen sein können. Zusätzlich sind in rot die extrapolierten Alter der Basis der SL-Einheiten H, F und C aufgelistet (berechnet auf der Grundlage von mittleren Sedimentationsraten für das MIS 1-5 Interval) (siehe auch Tab. 3). * = in den PW-Lagen ist eine Untergliederung in eine liegende „pink layer" und eine hangende „white layer" möglich; ** = die PW1-Lage ist von SCHULTE-LOH (2009) anhand eines Dolomit-Maximas identifiziert worden.

and the white layer W3 has an age of about 40 ka (POLYAK et al. 2004, 2009, ADLER et al. 2009). Furthermore, these authors propose MIS 5a and MIS 5e ages for the brown intervals B4 and B6/7, respectively (Fig. 5). In their age model, the identification of MIS 5a is based on the occurrence of the benthic foraminifer *Bulimina aculeata.* Using nannofossil stratigraphy, however, BACKMAN et al. (2009) proposed a different age model. Based on the prominent occurrence of *Emiliania huxleyi* and *Gephyrocapsa* spp. at 172 and 225 cm depth in core HLY0503-8JPC, the dark brown layers B5 and B6/7 are correlated with MIS 5a and 5e. The identification of MIS 5e (brown interval B7) in the record of core PS72/340-5 is supported by the dominance of planktic foraminifers and the presence of *N. pachyderma* dex. in the coarse fraction and the occurrence of coccoliths in smear slides (Fig. 7), interpreted as at least seasonally open-water conditions during the peak interglacial (cf. NØRGAARD-PEDERSEN et al. 2007a). Thus, the base of interval B7 interpreted as MIS 5/MIS 6 boundary

seems to be a quite reliable age fix point in our age model. In contrast to BACKMAN et al. (2009) and POLYAK et al. (2009) and in accordance with the age model of core PS51/38-4 (SPIELHAGEN et al. 2004), we propose a MIS 5d age for the pink-white layer PW2. At core PS51/38-4 (for location see Fig. 3), the PW2 layer coincides with prominent minima in the $\delta^{18}O$ and $\delta^{13}C$ records, interpreted as meltwater and IRD discharge during MIS 5d (Fig. 4; STEIN 2008, based on age model of SPIELHAGEN et al. 2004). Depending on the age model used, the horizon with very pale brown and pinkish, dolomite-rich clasts found at the base of brown interval B3, is dated to MIS 5/4 (about 75 ka; age model according to ADLER et al. 2009 and POLYAK et al. 2009) or MIS 4/3 (about 60 ka; age model according to BACKMAN et al. 2009) (Fig. 7).

The dominance of the very small *Gephyrocapsa* group in the 327-432 cm interval and the co-occurrence of genuine *E. huxleyi* at the 327 cm level at core HLY0503-8JPC suggest

111

that this section with dark brown intervals B9 and B10 was deposited during MIS 7 (BACKMAN et al. 2009). The identification of MIS 7.1 in the brown interval B9 of the record of core PS72/340-5 seems to be supported by the dominance of planktic foraminifers and the presence of *N. pachyderma* dex. in the coarse fraction and the occurrence of coccoliths in smear slides (Fig. 7), interpreted as at least seasonally open-water conditions typical for peak interglacial intervals (NØRGAARD-PEDERSEN et al. 2007a). Based on the lithostratigraphy of core PS72/392-5 (see Fig. 4 in STEIN et al. 2010, this vol.), the brown intervals B9 and B10 occur within SL unit K, which is dated to MIS 7 (Fig. 4), further supporting our age model. Thus, the overlying more sandy part of SL unit L is probably of MIS 6 age (Figs. 6, 7).

Below SL Unit K, the age model is still much more tentative and has to be proven by future studies (see also STEIN et al. 2010, this vol.). SL unit J with pink-white layer PW1 at its base is probably of MIS 8 age. A similar age for the PW1 layer ("near the MIS 8/7 boundary") has been published by KAUFMAN et al. (2008) and ADLER et al. (2009). If so, the underlying more sandy SL units H and F may be related to previous periods of extended ice sheets, i.e., the major glacials MIS 10 and 12, respectively (LISIECKI & RAYMO 2005). For unit G characterized by three prominent dark brown intervals (see Fig. 8 in STEIN et al. 2010, this vol.) and the first occurrence of calcareous foraminifers, an MIS 11 age is proposed. Assuming that the onset of sedimentation of sand-sized material coinciding with the lithologic Unit I/II boundary (Fig. 10), is related to the onset of IRD input, this change may correlate with the MIS 16 glaciation, the first of the "super" glaciations of the Pleistocene when benthic $\delta^{18}O$ values exceeded a critical threshold and excess ice was stored in Northern Hemisphere ice sheets (LISIECKI & RAYMO 2005; HODELL et al. 2008).

An additional, older stratigraphic marker also found in the HOTRAX cores from Mendeleev Ridge and the interior of the western Arctic Ocean, might be the top of predominantly dark brown sediments (POLYAK et al. 2009). This change to darker sediment colours coinciding with the boundary between SL units A and A1?, occurs in our cores from the eastern part of the northern transect at depths between of about 430 and 500 cm (Fig. 10) and is also reflected in a distinct drop in the lightness values (Fig. 11). To give an absolute age estimate remains difficult due to the lack of reliable age control. Based on extrapolation, POLYAK et al. (2009) give an estimate of "older than 500 ka". Using our mean sedimentation rates and extrapolation, the age of this colour change can be estimated to be older than about 750 ka.

Using the average sedimentation rates (MIS 1 to 5) for down-core extrapolation and age estimates in the cores from the northern transect (Tab. 3), the ages of the sandy SL units H and F, and especially SL unit C, would be younger than the proposed ages of MIS 10 (base 360 ka), MIS 12 (base 470 ka), and MIS 16 (base 660 ka), respectively. For the base of SL units H, F, and C, extrapolated ages would be about 290-340 ka, 400-470 ka, and 460-570 ka, respectively (Tab. 2). If our proposed ages (i.e., MIS 10, 12, and 16) are correct, this would imply that the sedimentation rates at times older than MIS 5 have to be lower than the MIS 1 to 5 mean values. Such reduced sedimentation rates in the older part seem to be not

Core	Area	0-PW2/ MIS 5d (0-110 ka)		0-Base B7/MIS 5 (0-130 ka)	
		thickness cm	LSR cm ky^{-1}	thickness cm	LSR cm ky^{-1}
PS72/340-5	Mendeleev Ridge	513	4.66	550	4.23
PS72/343-2	Mendeleev Ridge	589	5.35	650	5.00
PS72/344-3	Mendeleev Ridge	–	–	>803	>6.18
PS72/392-5	Mendeleev Ridge	59	0.54	68	0.52
PS72/396-5	Mendeleev Ridge	66	0.60	74	0.57
PS72/399-4	Mendeleev Ridge	71	0.65	84	0.65
PS72/404-4	Mendeleev Ridge	50	0.45	63	0.48
PS72/408-5	Mendeleev Ridge	100	0.91	114	0.88
PS72/410-3	Mendeleev Ridge	82	0.75	99	0.76
PS72/413-5	Mendeleev Ridge	92	0.84	111	0.85
PS72/418-7	Mendeleev Ridge	266	2.42	301	2.32
PS72/422-5	Mendeleev Ridge	221	2.01	252	1.94
HLY0503-8	Mendeleev Ridge	230	2.09	250	1.92
NP-26	Mendeleev Ridge	157	1.43	170	1.31
PS72/430-4	Makarov Basin	375	3.41	–	–
92BC-14	Northwind Ridge	335	3.05	–	–
92PC-30	Northwind Ridge	315	2.86	–	–
92PC-38	Northwind Ridge	220	2.00	–	–
92PC-40	Northwind Ridge	165	1.50	–	–
92BC-21	Northwind Ridge	70	0.64	-	–
PS51/38-4	Alpha Ridge	80	0.73	92	0.71
PS2185	Lomonosov Ridge	–	–	250	1.92
PS2754	Lomonosov Ridge	–	–	800	>6.15
PS2757	Lomonosov Ridge	–	–	615	4.73
PS2759	Lomonosov Ridge	–	–	610	4.69
PS2760	Lomonosov Ridge	–	–	447	3.44
PS2761	Lomonosov Ridge	–	–	470	3.62

Tab. 3: Mean sedimentation rates of intervals 0-110 ka (Interval from core top to depth of PW2 = base of SL Unit M = MIS 5d interval) and 0-130 ka (Interval from core top to base of brown interval B7 = base of MIS 5); see Table 2 for depths and thicknesses of key horizons. Numbers are based on the age model proposed here (see text for further details). In addition to data from the ARK-XXIII/3 cores, data from published cores are listed: Cores NP26 and HLY0503-8 (based on POLYAK et al. 2004, 2009, ADLER et al. 2009, but using an MIS 5d age for PW2). Northwind Ridge cores 92PC-30, 92PC-38, 92PC-40, and 93BC-21 (PHILLIPS & GRANTZ 2001; using an MIS 5d age for base of SL Unit M); Alpha Ridge Core PS51/038 (SPIELHAGEN et al. 2004; see Fig. 4); and Lomonosov Ridge Core PS2185 (SPIELHAGEN et al. 2004) and cores PS2754-8, PS2757-8, PS2759-8, PS2760-6, and PS2761-10 (STEIN et al. 1997, 2001).

Tab. 3: Mittlere Sedimentationsraten der Zeitintervalle 0-100 ka (Abschnitt von Kernoberfläche bis zur Tiefe der PW2-Lage = Basis der SL-Einheit M = MIS 5d) und 0-130 ka (Abschnitt von Kernoberfläche bis Tiefe des braunen Intervals B7 = Basis von MIS 5); siehe Tabelle 2 für Tiefenangaben und Mächtigkeiten der Leithorizonte. Die Berechnung der mittleren Sedimentationsraten erfolgte auf der Grundlage des hier postulierten Altersmodells. Zusätzlich zu den Daten der ARK-XXIII/3-Kerne sind publizierte Daten weiterer Arktis-Kerne aufgelistet: NP26 und HLY0503-8 (POLYAK et al. 2004, 2009, ADLER et al. 2009, aber mit MIS 5d-Alter für die PW2-Lage). Northwind-Rücken-Kerne 92PC-30, 92PC-38, 92PC-40 und 93BC-21 (nach PHILLIPS & GRANTZ 2001, aber mit MIS 5d-Alter für die Basis der SL-Einheit M); Alpha-Rücken-Kern PS51/038 (SPIELHAGEN et al. 2004; siehe Abb. 4); und Lomonosov-Rücken-Kerne PS2185 (SPIELHAGEN et al. 2004) und PS2754-8, PS2757-8, PS2759-8, PS2760-6, und PS2761-10 (STEIN et al. 1997, 2001).

unrealistic and supported by data from Lomonosov Ridge where a decrease in sedimentation rates at times older than MIS 6 was also identified (O'REGAN et al. 2008, POLYAK et al. 2009). Nevertheless, further data for improving our chronology is certainly needed (see MATTHIESSEN et al. 2010, this vol.).

Based on our age model, core PS72/340-5 probably contains

MIS 1 to MIS 8?, and cores PS72/343-2 and PS72/344-3 probably did not reach MIS 6 (Figs. 6, 7), whereas the cores from the northern transects recovered sediments probably older than MIS 16 (Fig. 10). Using the depth of pink-white layer PW2 (dated to MIS 5d) or the base of brown interval B7 (dated as MIS 5/6 boundary) (Tab. 2), average sedimentation rates reach values of 0.5-0.9 cm ky^{-1} in cores PS72/392-5 to PS72/413-5 (northern transect, top Mendeleev Ridge and Canadian side), increasing to 1.9 to 2.4 cm ky^{-1} at cores PS72/418-7 and PS72/422-5 (northern transect, Makarov Basin side) (Fig. 12, Tab. 3). At core PS72/430-4 (central Makarov Basin), average sedimentation rate even increases to 3.4 cm ky^{-1}. Along the southern transect, sedimentation rates are significantly higher reaching 4.2 to >6 cm ky^{-1} (Tab. 3).

This means that – not surprisingly – the sedimentation rates along the southern transect are significantly higher than those from the northern transect. A similar south-north decrease in sedimentation rates is also obvious in sediment cores from Northwind Ridge (Fig. 12; PHILLIPS & GRANTZ 2001). On Alpha Ridge, in the interior Arctic Ocean, very low sedimentation rates of about 0.2-0.7 cm ky^{-1} were determined (Figs. 4, 12). There is, on the other hand, a general increase in sedimentation rate from the Canada Basin across the Mendeleev Ridge toward the Makarov Basin along the northern transect, and this

increase continues further west towards southern Lomonosov Ridge where sedimentation rates >6.2 cm ky^{-1} were determined (Fig. 12, Tab. 3). Looking at the entire transect along about 80°30' N from the Canada Basin across Mendeleev Ridge and Lomonosov Ridge towards the Amundsen Basin, two areas can be separated: (i) The eastern area from the Canada Basin towards the crest of Mendeleev Ridge characterized by low sedimentation rates (<1 cm ky^{-1}) and influenced by the Beaufort Gyre system, and (ii) the area from the western flank of Mendeleev Ridge across the Makarov Basin towards Lomonosov Ridge characterized by significantly higher sedimentation rates (2 to >6 cm ky^{-1}) and influenced by the Transpolar Drift system (Fig. 12).

In the area from the Alaskan margin across Northwind Ridge and Mendeleev Ridge towards the interior of the western Arctic Ocean, POLYAK et al. (2009) already described the same south-north geographic pattern (decrease) of average late Quaternary sedimentation rates. According to these authors, Late Quaternary sedimentation in the western Arctic Ocean is mainly controlled by the combination of sea-ice concentration, and thus melt-out rates, and transportation distance from sediment sources at the continental margins. Thus, the lowest sedimentation rates of about 0.5 cm ky^{-1} or less occur on the ridges in the interior of the Amerasian Basin, caused by the combina-
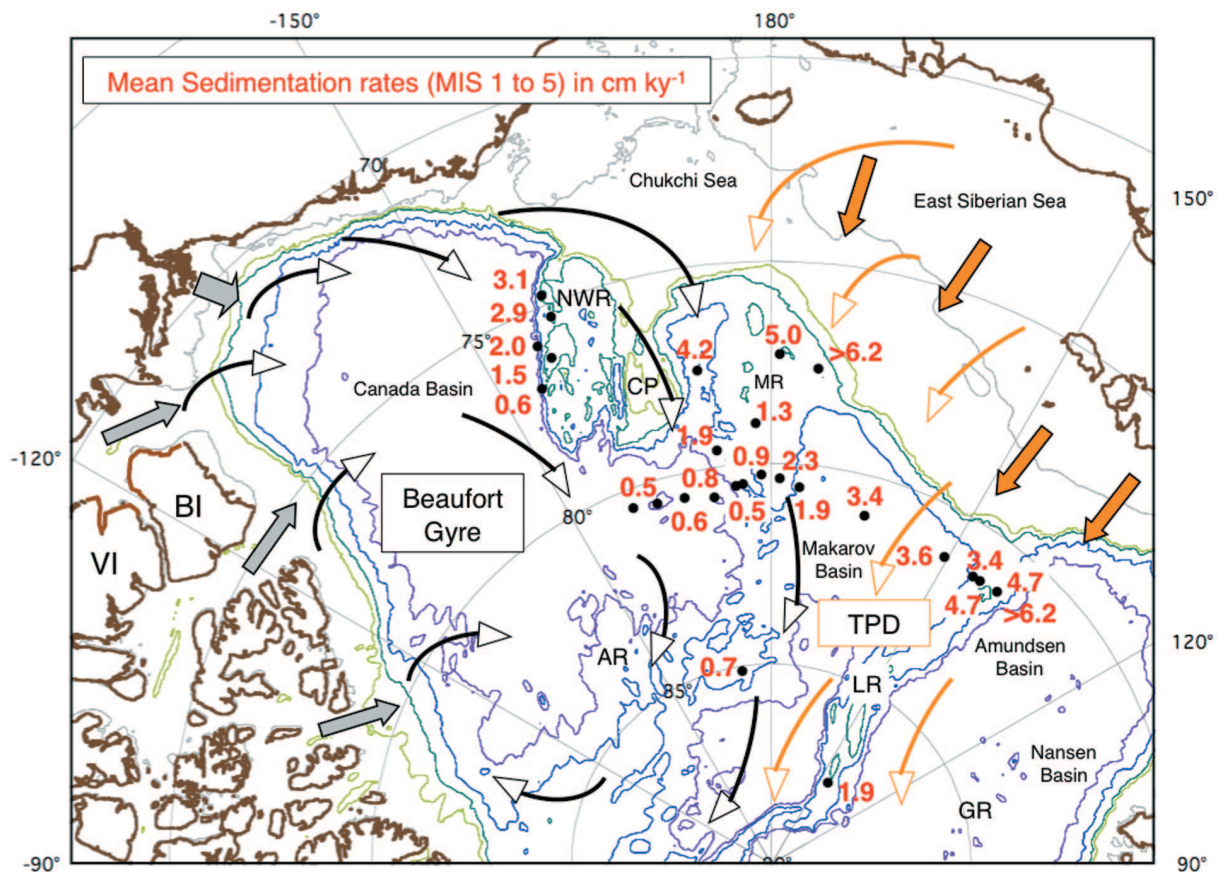

Fig. 12: Mean sedimentation rates of time interval MIS 1 to 5 in cm ky^{-1}. Sediment input and transport from North America via the Beaufort Gyre system and from Eurasia by the Transpolar Drift System (TPD) are indicated by gray/black and yellow arrows, respectively. NWR = Northwind Ridge, CP = Chukchi Plateau, AR = Alpha Ridge, MR = Mendeleev Ridge, LR = Lomonosov Ridge, GR = Gakkel Ridge, BI = Banks Island, VI = Victoria Island. For data base and references see Table 3.

Abb. 12: Mittlere Sedimentationsraten für den Zeitabschnitt MIS 1 bis MIS 5 in cm ky^{-1}. Sedimenteintrag und Transport von Nordamerika (Beaufort-Gyre-System) und Eurasien (TPD, Transpolardrift-System) sind als graue/schwarze bzw. rote/gelbe Pfeile angezeigt. NWR = Northwind-Rücken, CP = Chukchi-Plateau, AR = Alpha-Rücken, MR = Mendeleev-Rücken, LR = Lomonosov-Rücken, GR = Gakkel-Rücken, BI = Banks Island, VI = Victoria Island. Zu Daten und Quellen siehe Tabelle 3.

tion of highest sea-ice concentration and long transportation pathway in the Beaufort Gyre circulation system (POLYAK et al. 2009). In the area underneath the influence of the Transpolar Drift, on the other hand, sediment input from Eurasia, shorter transportation pathway, and less sea-ice concentration may have caused the higher sedimentation rates.

Quaternary history of Arctic ice sheets

Large parts of the land masses surrounding the Arctic Ocean were covered by ice sheets of variable size several times during the Quaternary (DYKE et al. 2002, SVENDSEN et al. 2004, EHLERS & GIBBARD 2007 and references therein; for LGM situation see Fig. 1). The detailed reconstruction of the history of these circum-Arctic ice sheets and its relationship to the paleoceanographic circulation pattern in the central Arctic Ocean is still under discussion, and major open questions concerning the timing (asynchronous versus synchronous evolution) and the extent of glaciations exist. Here, the study of carefully selected, continuous and dated marine sedimentary records from the continental slopes adjacent to glaciated shelves as well as from the deep-sea basins and ridges may help to decipher the history of continental glaciations. Once an ice sheet or glacier expands to the shoreline which may have extended close to the shelf break during glacial intervals of lowered sea level, icebergs are released which can drift toward the open ocean, carrying terrestrial IRD. Especially near the end of glacial maxima and during times of sea-level rise (e.g., glacial terminations), icebergs from extensive shelf glaciations could easily escape to the open Arctic Ocean (PHILLIPS &

GRANTZ 2001, SPIELHAGEN et al. 2004, ADLER et al. 2009). Thus, sediments containing pronounced sand and coarser-grain spikes are deposited during those times.

Looking at the northern transect across Mendeleev Ridge, the occurrence of sand and coarser-grain spikes indicative of IRD input are restricted to the upper part of the sedimentary sequences, i.e. lithological Unit I (Fig. 13). Contemporaneous with the onset of IRD, dolomite for the first time occurred in the sediments of core PS72/392-5 (Fig. 14). Dolomite-rich Paleozoic limestones are widespread in the Canadian Arctic and northern Greenland (Fig. 2; BISCHOF et al. 1996, VOGT 1997, PHILLIPS & GRANTZ 2001). These lithologies are characteristic for the near-coastal glacigenic sediments (glacial tills) of these areas as well. Thus, dolomite and its rock fragments are key indicators for identifying sediment input from northern Greenland and especially the Canadian Arctic with Banks and Victoria Islands that can be used as tracer for reconstruction of the history of the Laurentide Ice Sheet (LIS) (CLARK et al. 1980, DARBY et al. 1989, BISCHOF et al. 1996, VOGT 1997, PHILLIPS & GRANTZ 2001, NØRGAARD-PEDERSEN et al. 2007b).

Using our tentatitive age model, the first onset of dolomite sedimentation at core PS72/392-5 may have occurred within MIS 16, followed by major dolomite/IRD events during MIS 12 (SL unit F), 10 (SL unit H), and 8 (SL unit J). On the other hand, dolomite peaks were absent in MIS 6 (SL unit L), MIS 14, and prior to MIS 16 (Fig. 14). The first major distinct dolomite/IRD peak, i.e., diamicton deposition, occurred in SL unit F dated to MIS 12 and may suggest a first extreme extension of the LIS, as MIS 12 has been recognized as the most severe
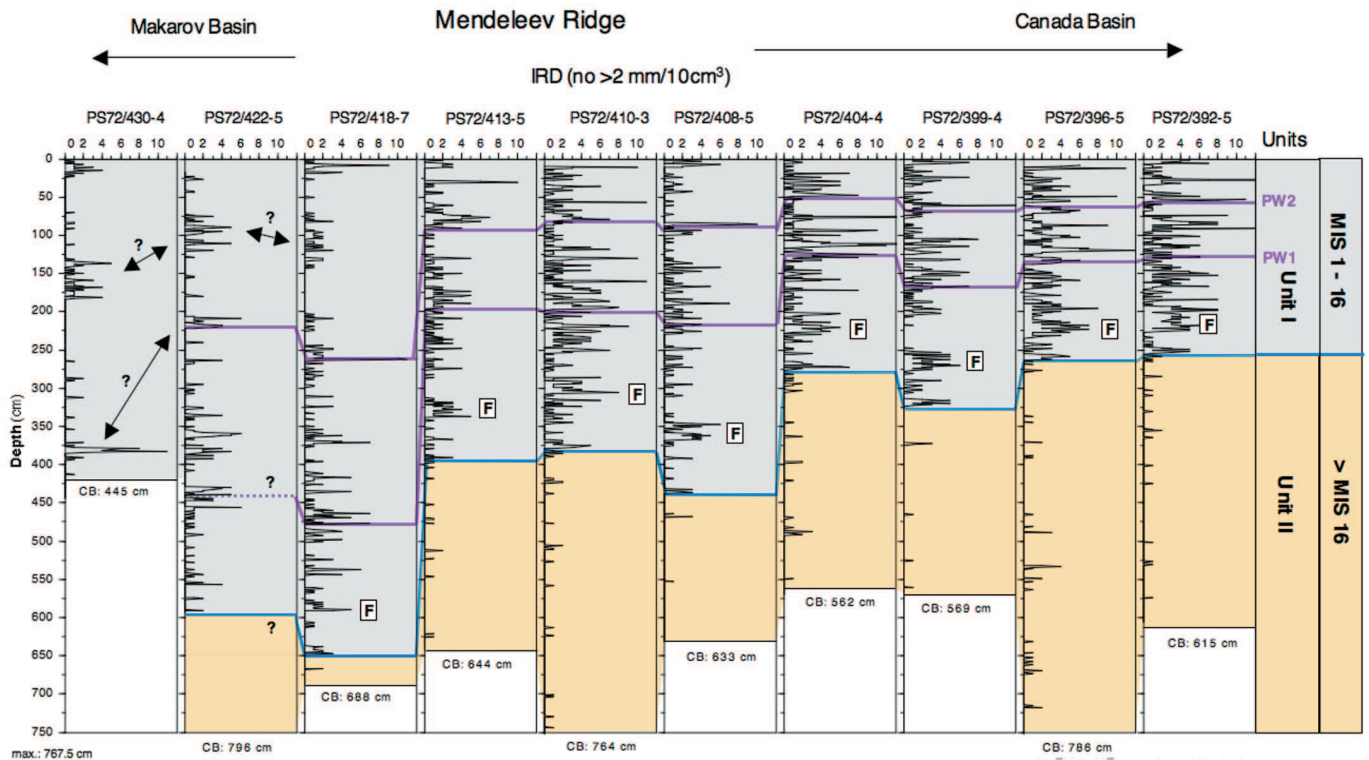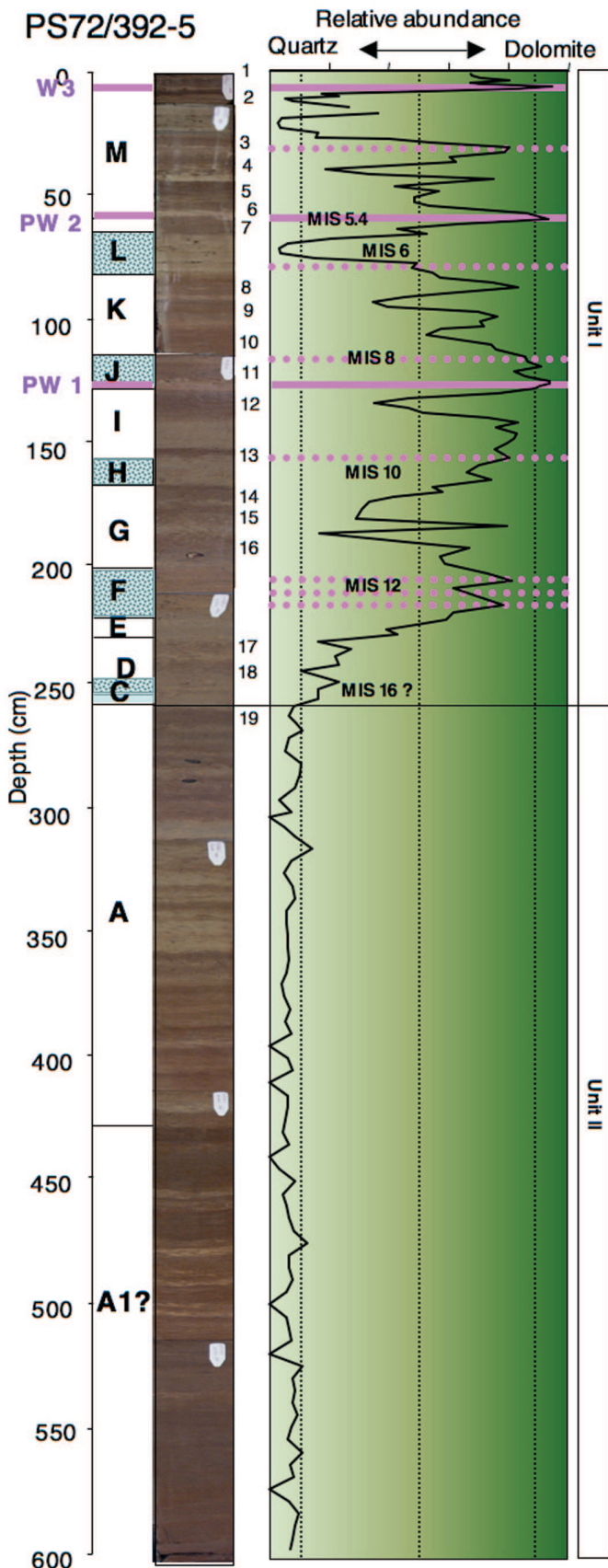

Fig. 13: Number of IRD grains >2 mm in sediment cores from the northern transect across the Mendeleev Ridge (for core locations see Fig. 3). The main pink-white layers PW1 and PW2, SL unit F (according to CLARK et al. 1980), and the Unit I/II boundary are indicated. According to the proposed preliminary age model, Unit I probably represents MIS 1 to 16.

Abb. 13: Anzahl der Eis transportierten Partikel >63 μm in Sedimentkernen vom nördlichen Transekt über den Mendeleev-Rücken. Die „pink-white layers" PW1 und PW2, die SL-Einheit F (nach CLARK et al. 1980) und die lithologischen Einheiten (Unit I und Unit II) sind angezeigt.

glaciation of the last 0.5 Ma (SHACKLETON 1987). If this interpretation is correct, this would imply a diachronous onset of major diamicton deposition in the Amerasian and Eurasian basins (SPIELHAGEN et al. 2004; for further discussion and alternate interpretation see MATTHIESSEN et al. 2010. this vol.).

Similar to the record of core PS72/392-5, prominent detrital carbonate (dolomite) layers – „Heinrich-like events" – were also recognized in North Atlantic sediments at IODP Sites U1308 and U1313 during MIS 8, 10, 12 and 16, but were absent from MIS 6 and 14 and in glacial periods prior to 640 ka (HODELL et al. 2008, STEIN et al. 2009a; for site location see Fig. 1). These events document episodes of enhanced iceberg delivery into the central mid-latitude North Atlantic due to sudden instability of the LIS and discharge of icebergs during the early and late (to deglacial) phase of major glaciations (cf., BROECKER & VAN DONK 1970, MCMANUS et al. 1999). HODELL et al. (2008) speculate that the ice volume (i.e. thickness) and the duration of glacial conditions surpassed a critical threshold during MIS 16 and activated the dynamical processes responsible for LIS instability. That means, based on the global benthic isotope record, ice sheets were reduced in thickness prior to MIS 16, and the duration of glacial periods may have been too short for a substantial fraction of the LIS to reach the pressure melting point. Thus, the detrital carbonate records from Arctic Ocean core PS72/392-5 and the Atlantic IODP sites may both reflect contemporaneous events of IRD input due to the disintegration events of the LIS, for the Arctic site a still speculative hypothesis that has to be approved by further studies.

For the last about 240 ka, a time interval with a much better age control, major periods of glaciations in North America and Eurasia were identified in sediments from the central Arctic Ocean. Based on a study of sediment cores from the Eurasian Basin, distinct maxima in IRD were recorded in uppermost MIS 7 to MIS 6 (190 to 130 ka), upper part of MIS 5 (substage 5b, about 90 to 80 ka), near the MIS 5/4 boundary (around 75 ka), and in the late MIS 4/early MIS 3 time interval (65 to 50 ka) (SPIELHAGEN et al. 2004), suggesting major continental glaciations in Scandinavia and Siberia during those times. Obviously, central Arctic sedimentation was not affected by the MIS 5d ice advance in the Svalbard/ Barents Sea area (MANGERUD et al. 1998).

On the Mendeleev Ridge at NP26 and HLY0503-8JPC cores (for location see Fig. 3), abundant carbonate rock fragments interpreted as IRD clasts with a LIS source, peak at the pink-white layers during MIS 8/7 (MIS 8 based on our age model), MIS 6/5 (MIS 5d based on our age model), MIS 4/3, and at about 40 ka (POLYAK et al. 2004, 2009). This Canadian source

Fig. 14: Standard lithostratigraphic (SL) units A1 to M (CLARK et al. 1980), core photographs showing the dark brown intervals (labeled 1 to 19 = B1 to B19), and relative dolomite versus quartz abundance of the sequence of Core PS72/392-5. These values were calculated as relative XRD intensity (RI) ratios: dolomite (2.89 Å peak) / (dolomite (2.89 Å peak) + quartz (4.26 Å peak)). For data source and details see STEIN et al. (this vol.).
Dolomite maxima (coinciding with IRD maxima; see Fig. 13) are related to sediment (IRD) input from the Laurentide Ice Sheet area, whereas quartz maxima may represent supply from Eurasian sources (see text for further discussion). The main pink-white (PW1 and PW2) and white (W3) layers are indicated by pink bars, pink-coloured dotted lines indicate occurrence of horizons with pinkish lenses/clasts. Proposed MIS ages based on a preliminary age model, are shown as well.

Abb. 14: Lithostratigraphische Standard (SL)-Einheiten A1 bis M nach Kern - Fotographien mit braunen Lagen B1 bis B19, und relative Dolomit/Quarz-Häufigkeit in Kern PS72/392-5. Die Dolomit/Quarz-Werte sind aus den relativen XRD-Intensitäten berechnet worden (siehe STEIN et al. dieses Heft). Die angegebenen Marinen Isotopen Stadien (MIS) basieren auf dem vorläufigen Altersmodell.

of IRD is also supported by distinct Fe oxid spikes from a Laurentide source, characterizing the pink-white layers (POLYAK et al. 2004). The most prominent pinkish intervals characterized by high numbers of dolomitic IRD/dropstones, are also recovered at core PS72/340-5 (Fig. 7) as well as all other cores on the northern transect (Fig. 10). Based on our age model, these IRD events are related to increased IRD supply due to extended glaciations in Arctic Canada during MIS 8(/7), MIS 5d, and MIS 4/3. During MIS 5d, a pink-white layer was even found in the Alpha Ridge core PS51/038-4 (Fig. 4) as well as on Lomonosov Ridge at cores PS2185 and PS70/358 (see STEIN et al. 2010, this vol.; for location see Fig. 3). During interglacials MIS 7 and the middle part of MIS 5 as well as during the last about 20 ka, also increased amount of detrital carbonate was determined in the record of core PS2185 (SPIELHAGEN et al. 1997, using the stratigraphy of SPIELHAGEN et al. 2004). Detrital carbonate is related to a sediment source in the Canadian Arctic, suggesting substantial sediment transport towards the Eurasia Basin by an extended Beaufort Gyre at those (mainly interglacial) time intervals (PHILLIPS & GRANTZ 2001).

Besides IRD peaks coinciding with high dolomite content, ADLER et al. (2009) described some IRD peaks in the HLY0503-8JPC sequence that are composed primarily of quartz grains and dated into MIS 4 and mid-MIS 3 as well as near the top of MIS 6 and MIS 8. Intervals with increased quartz content were also identified in MIS 3 and MIS 6 (see Fig. 14) as well as in the older sandy intervals (Clark's SL units J, H, F, and C) of core PS72/392-5 (STEIN et al. 2010, 2010, this vol.). Quartz, a major to dominant mineral in central Arctic Ocean sediments, is especially enriched in sediments with a dominantly Eurasian provenance (SPIELHAGEN et al. 1997, POLYAK et al. 2004). When using quartz as provenance indicator, however, one should have in mind that quartz may also derive from the Canadian Arctic, that is, the southwestern Canadian Archipelago and parts of northern Canada from south of Amundsen Gulf to the Canadian/Alaskan border, where similar quartz contents were determined (Fig. 2; BISCHOF et al. 1996, VOGT 1997, PHILLIPS & GRANTZ 2001). An increased input from Eurasia would imply that circulation during some glacial periods was probably different from the present Beaufort Gyre-dominated system in the western ArcticOcean (DARBY et al. 2002, POLYAK et al. 2004, 2009). Another possible explanation for Eurasian glacial material found on Mendeleev Ridge, however, could also be the existence of larger ice sheets at the eastern Eurasian margin (the East-Siberian shelf) as proposed by GROSSWALD (1980) three decades ago. Recently, speculations on this hypothesis, i.e., the existance of widespread circum-Arctic glaciations, started again (POLYAK et al. 2001, 2009, JAKOBSSON et al. 2008, ADLER et al. 2009). This hypothesis, however, has to be proven by data. In this context, the data and material from our "Polarstern" ARK-XXIII/3 expedition may give new insights.

New speculations and discussions on large-sized glaciations and ice shelves were initiated by the results of detailed geophysical seafloor mapping in the Arctic Ocean from nuclear submarines and icebreakers, that identified a wide variety of glaciogenic geomorphic features at water depths down to 1000 m, including iceberg keel scours, most abundant at water depths shallower than ~350-400 m, and flutes and megascale glacial lineations extending as deep as ~1000 m

below the present sea level (JAKOBSSON 1999, POLYAK et al. 2001, JAKOBSSON et al. 2008 *cum lit.*). The lineated areas are typically associated with large-scale seafloor erosion, accentuated by a conspicuous truncation of pre-glacial strata capped with a mostly thin layer of diamict sediment, in which the lineations are formed (JAKOBSSON et al. 2008, DOWDESWELL et al. 2004). Major erosional events on Lomonosov Ridge and the Chukchi Borderland (two events) have been dated to MIS 6 (JAKOBSSON et al. 2001), and to the LGM and the time interval between MIS 4 and MIS 5d (POLYAK et al. 2007), respectively. In HOTRAX-05 cores from Northwind Ridge, a third event represented in a diamicton of a MIS 6 age, was determined (DARBY et al. 2005). Although the exact mechanisms, timing and provenance of these ice masses are not yet well understood and still discussed controversely (POLYAK et al. 2001, KRISTOFFERSEN et al. 2004, JOKAT 2005), these data indicate that very large glacial ice masses extended into the central Arctic Ocean from surrounding North American and Eurasian ice sheets several times during the Quaternary.

JAKOBSSON et al. (2008) gave two mechanisms of glacial impact on the Chukchi Borderland causing the widespread erosion: (i) large-scale erosion by ice masses overriding the Chukchi Borderland from the east and southeast and related to floating ice masses (ice shelves) propelled by ice major streams of the LIS (DYKE et al. 2002, STOKES et al. 2005), and
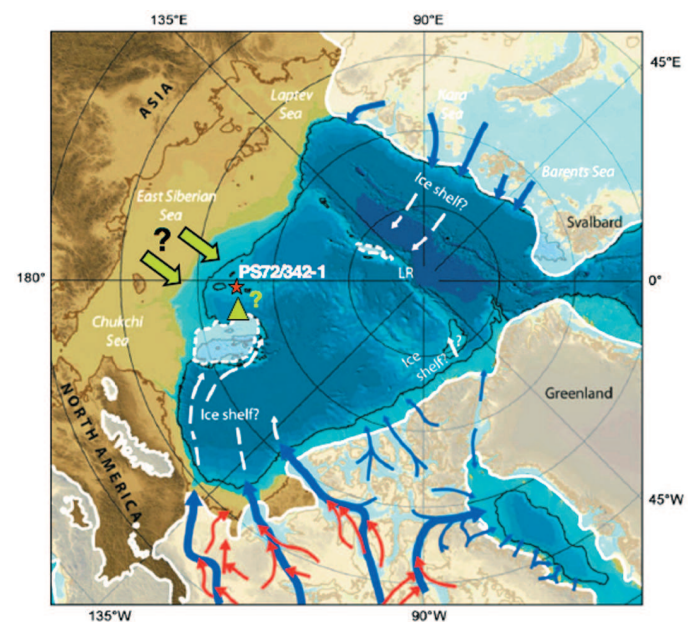

Fig. 15: Bathymetric map of the Arctic Ocean modified to show conditions of lowered sea level by 120 m during LGM maximum glaciation. Limits of the Eurasian and North American ice sheets according to SVENDSEN et al. (2004) and DYKE et al. (2002), respectively; main ice streams (blue arrows) according to DE ANGELES & KLEMAN (2005) and KLEMAN & GLASSER (2007). Red arrows show ice stream tributaries and episodic diversions of ice stream drainage within main ice stream corridors. Projected flow lines of ice shelves and limits of ice rises are mapped based on interpretation of observed glaciogenic seafloor bedforms (Figure from JAKOBSSON et al. 2008, supplemented). Red star indicates location of Core PS72/342-1 on Mendeleev Ridge, green triangle and arrows show proposed alternate flow lines of ice streams that may have caused diamicton formation at core location (cf. Figs. 16 and 17).

Abb. 15: Modifizierte bathymetrische Karte des Arktischen Ozeans zur Zeit des letzten glazialen Maximums mit einem 120 m abgesenkten Meeresspiegel. Ausdehnung der eurasischen und nordamerikanischen Eisschilde nach SVENDSEN et al. (2004) bzw. DYKE et al. (2002), Eisströme (blaue Pfeile) nach DE ANGELES & KLEMAN (2005) und KLEMAN & GLASSER (2007). Abbildung ergänzt nach JAKOBSSON et al. 2008.

(ii) impact of an ice cap centred over the plateau or the entire borderland (Fig. 15). A similar erosional event by grounding of large ice masses (ice rise?) may also have occurred on the southern part of Mendeleev Ridge, as reflected in a prominent diamicton identified in water depths between about 800-900 m (Fig. 16). Distinct erosional structures are obvious at the base of the diamiction. The top about one metre of the diamicton could by sampled by core PS72/342-1. These sediments are more stiff and homogeneous and characterized by increased wet bulk density and increased shear strength values (Fig. 17). Based on correlation to core PS72/340-5 and our tentative age model, the age of this erosional event should be within MIS 5 (stadial MIS 5b or 5d?) (or older) and, thus, may have been contemporaneous with the event on the Chukchi Borderland (MIS 4-MIS 5d; POLYAK et al. 2007). Whether the grounding ice masses on the southern Mendeleev Ridge were related to floating ice masses from the LIS/Chukchi Borderland or perhaps from an East Siberian ice shelf (Fig. 15) has to be proven by further studies considering more sediment cores as well as subbotom sediment acoustic (PARASOUND) and multi-channel seismic data (NIESSEN et al. 2010, this vol.).

CONCLUSIONS

First results of studies of sediment cores recovered during the "Polarstern" ARK-XXIII/3 expedition at Mendeleev Ridge allow the following conclusions:

(1) Based on the visual core description, the standard lithological (SL) units A to M developed by CLARK et al. (1980), could also be clearly identified in sediment cores from the transect along 80°30'N across Mendeleev Ridge. Following CLARK et al. (1980), the content of sand-sized material (enriched in SL units C, F, H, J, L, and parts of M) and the pink-white layers were considered to be the key sedimentary characteristics used for core correlation and – together with the prominent (dark) brown intervals – for developing a preliminary age model.

(2) The most distinct pinkish intervals characterized by high numbers of dolomitic IRD (large-sized dropstones), are related to increased IRD supply due to disintegration of an extended Laurentide Ice Sheet (LIS) during MIS 8(/7), MIS 5d, and MIS 4/3. Pink-white horizons (and layers with enrich-
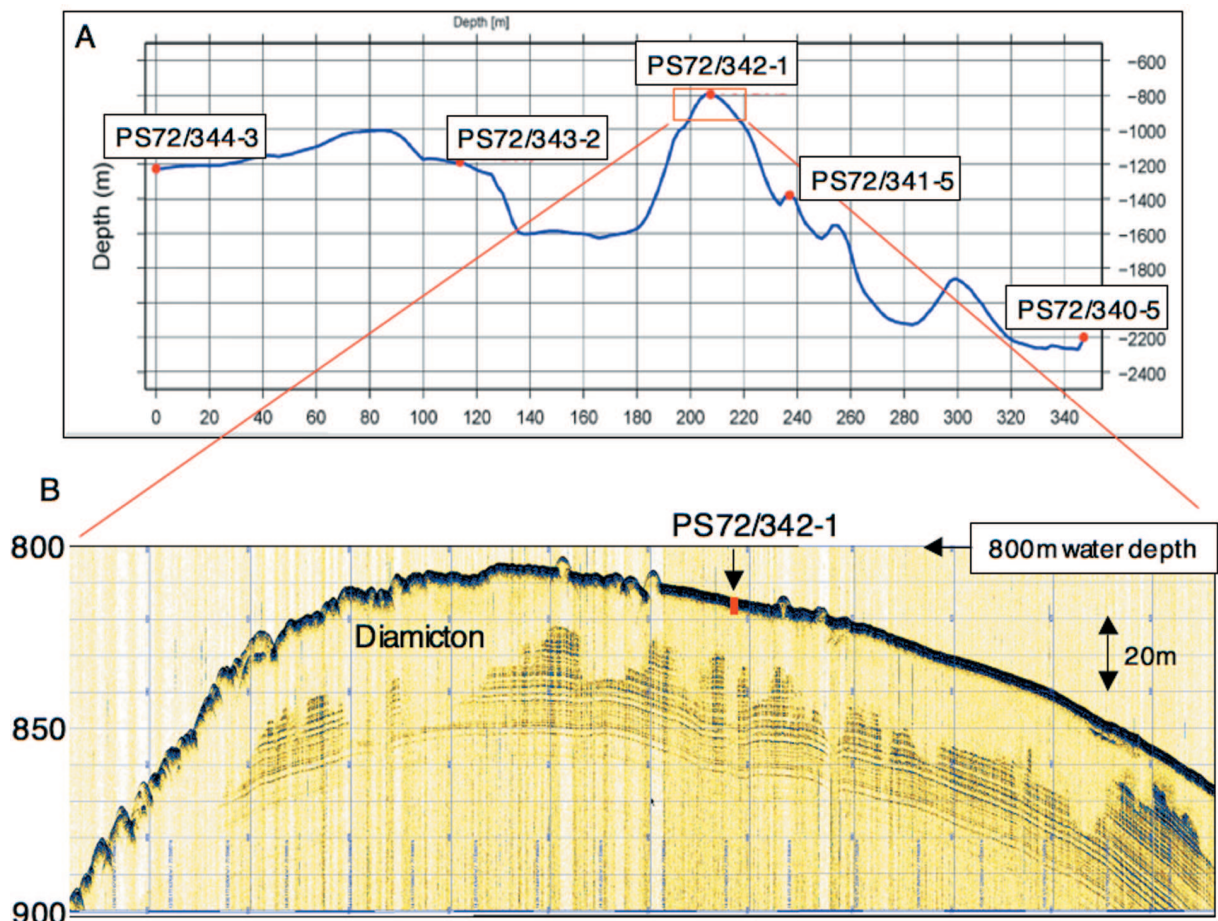

Fig. 16: (A) Southern transect across Mendeleev Ridge with geological sampling stations carried out during "Polarstern" expedition ARK-XXIII/3. For location see Figure 3.
(B) Detail of PARASOUND subbottom profile across the location of core PS72/342-1, showing a thick near-surface transparent (diamicton) unit with erosional structures at the base and possible iceberg scouring at the seafloor.

Abb. 16: Südlicher Transekt über den Mendeleev-Rücken mit geologischen Proben-Stationen der "Polarstern"-Expedition ARK-XXIII/3. Zu Lokationen siehe Abbildung 3.
(B) Detail des PARASOUND-Sedimentprofils über der Kernstation PS72/342-1 mit deutlichen Erosionsstrukturen an der Basis des oberflächen-nahen akustisch transparenten Diamiktons und Eisberg-Schleifspuren am Meeresboden.
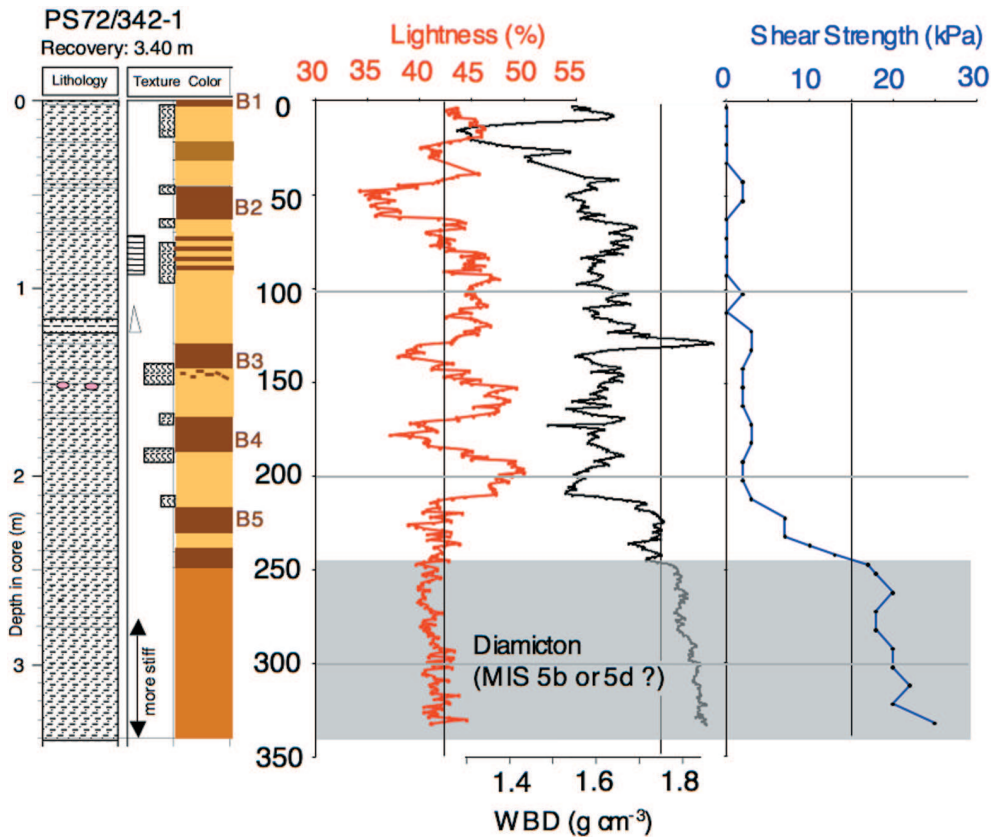
Fig. 17: Core PS72/342-1 from southern Mendeleev Ridge (for Location see Fig. 3). Simplified summary of lithology, main sediment colours with brown to dark brown intervals B1 to B5, lightness (red curve), wet bulk density (WBD, black curve), and shear strength (blue curve). Gray bar indicates diamicton-type sediment characterized by distinctly increased uniform density, shear strength and stiffness. Based on the proposed tentative age model, the diamicton is older than MIS 5a (MIS 5b or MIS 5d?).

Abb. 17: Kern PS72/342-1 vom südlichen Mendeleev-Rücken. Vereinfachtes Schema der Lithologie, der Sedimentfarben mit braunen Intervallen B1 bis B5, Helligkeit (L*, rote Kurve), Nassdichte (WBD, schwarze Kurve) und Scherfestigkeit (blaue Kurve). Grau markiert ein Diamikt mit sehr gleichmäßigen Messwerten. Nach dem neuen Altersmodell ist der Diamikt älter als MIS 5a (vermutlich MIS 5b oder MIS 5d?).

ment of pink-white lenses/clasts), however, were found more often than those described by CLARK et al. (1980), suggesting that surges of icebergs with a LIS origin may have occurred more frequently.

(3) Using our tentatitive age model, the first onset of dolomite sedimentation at Core PS72/392-5 may have occurred within MIS 16, followed by major dolomite events during MIS 12, 10, and 8. On the other hand, dolomite peaks were absent in MIS 6 and 14 and prior to MIS 16. The first major distinct dolomite peak found in SL Unit F and dated to MIS 12, may suggest a first extreme extension of the LIS and a diachronous onset of diamicton deposition in the Amerasian and Eurasian basins. The IRD peaks and detrital-carbonate maxima may reflect events of IRD input due to the disintegration events of the LIS at the end of MIS 8, 10, 12, and 16, a still speculative hypothesis that has to be approved by further studies. That means, at this stage of investigation a change in oceanic circulation pattern cannot be excluded as an alternative explanation for the onset of dolomite sedimentation at the study sites.

(4) Looking at the entire transect along about 80°30' N from the Canada Basin across Mendeleev Ridge and Lomonosov Ridge towards the Amundsen Basin, two areas can be separated:
(i) The eastern area from the Canada Basin towards the crest of Mendeleev Ridge characterized by low sedimentation rates (<1 cm ky^{-1}) and influenced by the Beaufort Gyre system, and
(ii) the area from the western flank of Mendeleev Ridge across the Makarov Basin towards Lomonosov Ridge characterized by significantly higher sedimentation rates (2- >6 cm ky^{-1}) and influenced by the Transpolar Drift system.

(5) A diamicton with erosional structures at its base was identified on southern Mendeleev Ridge in water depths of 800-900 m, suggesting the impact of grounding ice masses.

Future research of this unique new core material recovered during the "Polarstern" ARK-XXIII/3 expedition will help to solve some of the problems in Arctic Ocean stratigraphy/ chronology and paleoenvironmental reconstructions. Multi-proxy investigations – partly in combination with the evaluation of the PARASOUND profiles – will allow identifications of main source regions and major transport processes of terrigenous matter, reconstructions of circum-Arctic ice-sheet extension and history, oceanic currents, surface-water productivity, and sea-ice cover, and estimates of sedimentary budgets.

Montréal, Québec, Canada,
David Poggemann, Leibniz Institute for Marine Sciences IFM-
GEOMAR, Kiel University, 24148 Kiel,
participated in the ARK-XXIII/3 expedition and contributed to
the data collected onboard RV "Polarstern" and presented in
this paper.

References

ACIA (2004): Arctic Climate Impact Assessment – Impacts of a Warming Arctic.- Cambridge University Press, 1-1042.

Adler, R.E., Polyak, L., Ortiz, J.D., Kaufman, D.S., Channell, J.E.T., Xuan, C., Grottoli, A.G., Sellén, E. & Crawford, K.A. (2009): Sediment record from the western Arctic Ocean with an improved Late Quaternary age resolution: HOTRAX core HLY0503-8JPC, Mendeleev Ridge.- Global Planet. Change 68: 18-29.

Aksu, A.E. & Mudie, P.J. (1985): Magnetostratigraphy and palynology demonstrate at least 4 million years of Arctic sedimentation.- Nature 318: 280-283.

Backman, J., Fornaciari, E. & Rio, D. (2009): Biochronology and paleoceanography of late Pleistocene and Holocene calcareous nannofossil abundances across the Arctic Basin. Mar. Micropal. 72: 86-98.

Backman, J., Jacobsson, M., Knies, J., Knudsen, J., Kristoffersen, Y., Lif, A., Musatov, E. & Stein, R. (1997): Geological coring and high resolution chirp sonar profiling.- Cruise report, Polarforskningssekretaariatets arsbok 1995/96, Stockholm, 64-66.

Backman, J., Jakobsson, M., Løvlie, R., Polyak, L. & Febo, L.A. (2004): Is the central Arctic Ocean a sediment starved basin?- Quat. Sci. Rev. 23: 1435-1454.

Behrends, M. (1999): Reconstruction of sea-ice drift and terrigenous sediment supply in the Late Quaternary: heavy-mineral associations in sediments of the Laptev-Sea continental margin and the central Arctic Ocean.- Reps. Pol. Res. 310: 1-167.

Bischof, J., Clark, D. & Vincent, J. (1996): Pleistocene paleoceanography of the central Arctic Ocean: the sources of ice rafted debris and the compressed sedimentary record.- Paleoceanography 11: 743-756.

Bischof, J.F. & Darby, D.A. (1997): Mid to Late Pleistocene ice drift in the western Arctic Ocean: evidence for a different circulation in the past.- Science 277: 74-78.

Brigham-Grette, J., Hopkins, D.M., Ivanov, V.F., Basilyan, A.E., Benson, S.L., Heiser, P.A. & Pushkar, V.S. (2001): Last Interglacial (isotope stage 5) glacial and sea-level history of coastal Chukotka Peninsula and St. Lawrence Island, Western Beringia.- Quat. Sci. Rev. 20: 419-436.

Channell, J.E.T., Kanamatsu, T., Sato, T., Stein, R., Alvarez Zarikian, C.A., Malone, M.J. & the Expedition 303/306 Scientists (2006a): Proceedings of the Intergrated Ocean Drilling Program, Vol 303/306 Expeditions Report, North Atlantic Climate, doi: 10.2204/iodp.proc.303306.2006.

Channell, J.E.T. & Xuan, C. (2009): Self-reversal and apparent magnetic excursions in Arctic sediments.- Earth Planet. Sci. Lett. 284: 124-131.

Clark, D.L. (1970): Magnetic reversals and sedimentation rates in the Arctic Basin.- Geol. Soc. Amer. Bull. 81: 3129-3134.

Clark, D.L. (1996): The Pliocene record in the central Arctic Ocean.- Mar. Micropaleontol. 27: 157-164.

Clark, D.L., Whitman, R.R., Morgan, K.A. & Mackey, S.D. (1980): Stratigraphy and glacialmarine sediments of the Amerasian Basin, central Arctic Ocean.- Geol. Soc. Amer. Spec. Pap. 181: 1-57.

Clark, D.L., Chern, L.A., Hogler, J.A. Mennicke, C.M. & Atkins, E.D. (1990): Late Neogene climate evolution of the central Arctic Ocean.- Mar. Geol. 93: 69-94.

Clark, D.L., Whitman, R.R., Morgan, K.A. & Mackey, S.D. (1980): Stratigraphy and glacialmarine sediments of the Amerasian Basin, central Arctic Ocean.- Geol. Soc. Amer. Spec. Pap. 181: 1-57.

Darby, D.A. (2003): Sources of sediment found in sea ice from the western Arctic Ocean, new insights into processes of entrainment and drift patterns.- J. Geophy. Res. 108, C8, 3257, doi:10.1029/2002JC001350.

Darby, D.A. & Bischof, J.F. (2004): A Holocene record of changing Arctic Ocean ice drift, analogous to the effects of the Arctic Oscillation.- Paleoceanography doi:10.1029/2003PA000961.

Darby, D.A., Bischof, J.F. & Jones, G.A. (1997): Radiocarbon chronology of depositional regimes in the western Arctic Ocean.- Deep Sea Res. II 44(8): 1745-1757.

Darby, D.A., Bischof, J.F., Spielhagen, R.F., Marshall, S.A. & Herman, S.W. (2002): Arctic ice export events and their potential impact on global climate during the late Pleistocene.- Paleoceanography 17 (2) doi:10.1029/2001PA000639.

Darby, D.A., Jakobsson, M. & Polyak, L. (2005): Icebreaker expedition collects key Arctic seafloor and ice data.- Eos 86 (52): 549-552.

Darby, D.A., Naidu, A.S., Mowatt, T.C. & Jones, G. (1989): Sediment composition and sedimentary processes in the Arctic Ocean.- In: Y. HERMAN (ed), The Arctic Seas - Climatology, Oceanography, Geology, and Biology.- Van Nostrand Reinhold Co., New York, 657-720.

Darby, D.A., Polyak, L. & Bauch, H. (2006): Past glacial and interglacial conditions in the Arctic Ocean and marginal seas - a review.- Progress Oceanogr. 71: 129-144.

De Angeles, H. & Kleman, J. (2005): Palaeo-ice streams in the northern Keewatin sector of the Laurentide Ice Sheet.- Annals Glaciol. 42: 135-144.

Dickson, R.R., Osborn, T.J., Hurrell, J.W., Meincke, J., Blindheim, J., Adlandsvik, B., Vinje, T., Alekseev, G. & Maslowski, W. (2000): The Arctic Ocean response to the North Atlantic Oscillation.- J. Climat. 13(15): 2671-2696.

Dowdeswell, J.A., Ó Cofaig, C. & Pudsey, C.J. (2004): Thickness and extent of the subglacial till layer beneath an Antarctic paleo-ice stream.- Geology 32: 13-16.

Dyke, A.S., Andrews, J.T., Clark, P.U., England, J.H., Miller, G.H., Shaw, J. & Veillette, J.J. (2002): The Laurentide and Innuitian ice sheets during the last glacial maximum.- Quat. Sci. Rev. 21: 9-31.

Ehlers, J. & Gibbard, P.L. (2007): The extent and chronology of Cenozoic global glaciation.- Quat. Internat. 164-165, 6-20.

England, J.H., Furze, M.F.A. & Doup, J.P. (2009): Revision of the NW Laurentide Ice Sheet: Implications for paleoclimate, the northeast extreminty of Beringia, and Arctic Ocean sedimentation.- Quat. Sci. Rev. 28: 1569-1810.

Fütterer, D.K. (1992): ARCTIC'91: The Expedition ARK-VIII/3 of RV "Polarstern" in 1991.- Rep. Pol. Res. 107: 1-267.

Grantz, A., Clark, D.L., Phillips, R.L. & Srivastava, S.P. (1998): Phanerozoic stratigraphy of Northwind Ridge, magnetic anomalies in the Canada Basin, and the geometry and timing of rifting in the Amerasia Basin, Arctic Ocean.- Geol. Soc. Amer. Bull. 110: 801-820.

Grobe, H. (1987): A simple method for the determination of ice-rafted debris in sediments cores.- Polarforschung 57: 123-126.

Grosswald, M.G. (1980): Late Weichselian ice sheets of northern Eurasia.- Quat. Res. 13: 1-32.

Hodell, D.A., Channell, J.E.T., Curtis, J.H., Romero, O.E. & Röhl, U. (2008): Onset of Heinrich Events in the Eastern North Atlantic at the end of the Middle Pleistocene Transition (~640 ka)?.- Paleoceanography, doi:10.1029/2008PA001591.

Hurrell, J.W. (1995): Decadal trends in the North Atlantic oscillation: Regional temperatures and precipitation.- Science 269: 676-679.

Intergovernmental Panel on Climate Change (IPCC) (2007): Climate Change 2007 - Fourth Assessment Report.- Cambridge University Press, Cambridge.

Jackson, H.R., Mudie, P.J. & Blasco, S.M. (1985): Initial geological report on CESAR -The Canadian Expedition to study the Alpha Ridge, Arctic Ocean.- Geol. Surv. Can. Pap. 84-22: 1-177.

Jakobsson, M. (1999): First high-resolution chirp sonar profiles for the central Arctic Ocean reveal erosion of Lomonosov Ridge sediments.- Mar. Geol. 158: 111-123.

Jakobbsson, M., Polyak, L., Edwards, M., Kleman, J. & Coakley, B. (2008): Glacial geomorphology of the Central Arctic Ocean: The Chukchi Borderland and the Lomonosov Ridge.- Earth Surface Proc. Landforms 33: 526-545.

Jakobsson, M., Backman, J., Murray, A. & Løvlie, R. (2003): Optically stimulated luminescence dating supports central Arctic Ocean cm-scale sedimentation rates.- Geochem. Geophys. Geosyst. 4: 1-11.

Jakobsson, M., Løvlie, R., Al-Hanbali, H., Arnold, E., Backman, J. & Mörth, M. (2000): Manganese and color cycles in Arctic Ocean sediments constrain Pleistocene chronology.- Geology 28: 23-26.

Jakobsson, M., Løvlie, R., Arnold, E.M., Backman, J., Polyak, L., Knutsen, J.-O. & Musatov, E. (2001): Pleistocene stratigraphy and paleoenvironmental variation from Lomonsov Ridge sediments, central Arctic Ocean.- Global Planet. Change 31: 1-22.

Jakobsson, M., Polyak, L. & Darby, D.A. (2007): Arctic Ocean: Glacial history from multibeam mapping and coring during HOTRAX (2005) and LOMROG (2007).- EOS Trans. 88 (52), AGU Fall Meet. Suppl. Abstract PP42B-06.

Jokat, W. (ed) (1999): Arctic'98: The Expedition ARK-XIV/1a of RV Polarstern in 1998.- Rep. Pol. Res. 308: 1-159.

Jokat, W. (ed) (2009): The Expedition ARK-XXIII/3 of RV Polarstern in 2008.- Rep. Pol. Mar. Res. 597: 1-221.

Jokat, W. (2005): The sedimentary structure of the Lomonosov Ridge between 88° N and 80° N.- Geophys. J. Internat. 163: 698-726.

Jokat, W., Stein, R., Rachor, E. & Schewe, I. (1999): Expedition gives fresh view of central Arctic geology.- EOS Trans. 80: 465 + 472-473.

Jones, G.A. (1987): The central Arctic Ocean sediment record: current progress in moving from a litho- to a chronostratigraphy.- Pol. Res. 5: 309-311.

Kaufman, D.S., Polyak, L., Adler, R., Channell, J.E.T. & Xuan, C. (2008): Dating late Quaternary planktonic foraminifer Neogloboquadrina pachyderma from the Arctic Ocean using amino acids.- Paleoceanography 23,

PS3224, doi:10.1029/2008PA001618.

Kleman, J. & Glasser, N.F. (2007): The subglacial thermal organisation (STO) of ice sheets.- Quat. Sci. Rev. 26: 585-597.

Knies, J., Kleiber, H.P., Matthiessen, J., Müller, C. & Nowaczyk, N. (2001): Marine ice-rafted debris records constrain maximum extent of Saalian and Weichselian ice-sheets along the northern Eurasian margin.- Global Planet. Change 31: 45-64.

Knies, J., Müller, C., Nowaczyk, N., Vogt, C. & Stein, R. (2000): A multiproxy approach to reconstruct the environmental changes along the Eurasian continental margin over the last 150 kyr.- Mar. Geol. 163: 317-344.

Kristoffersen, Y., Coakley, B., Jokat, W., Edwards, M., Brekke, H. & Gjengedal, J. (2004): Seabed erosion on the Lomonosov Ridge, central Arctic Ocean: a tale of deep draft icebergs in the Eurasia Basin and the influence of Atlantic water inflow on iceberg motion?.- Paleoceanography 19: PA3006.

Lisiecki, L.E. & Raymo, M.E. (2005) A Pliocene-Pleistocene stack of 57 globally distributed benthic ?18O records.- Paleoceanography 20: PA1003, doi:10.1029/2004PA001071.

Lund, S., Stoner, J.S., Channell, J.E.T. & Acton, G. (2006): A summary of Brunhes paleomagnetic field variability recorded in Ocean Drilling Program cores.- Phys. Earth Plan. Internat. 156: 194-204.

Macdonald, R.W., Harner, T., Fyfe, J., Loeng, H. & Weingartner, T. (2003): AMAP Assessment 2002: The Influence of Global Change on Contaminant Pathways to, within, and from the Arctic.- Arctic Monitoring and Assessment Programme (AMAP), Oslo, Norway. xii+ 1-65.

Martinez, N.C., Murray, R.W., Dickens, G.R. & Kölling, M. (2009): Discrimination of sources of terrigenous sediment deposited in the central Arctic Ocean through the Cenozoic.- Paleoceanograpgy 24: PA1210, doi:10.1029/2007PA001567.

Minicucci, D.A. & Clark, D.L. (1983): A Late Cenozoic stratigraphy for glacial-marine sediments of the eastern Alpha Cordillera, central Arctic Ocean.- In: B.F. MOLNIA (ed), Glacial-marine sedimentation.- Plenum Press, New York, 331-365.

Mudie, P.J. & Blasko, S.M. (1985): Lithostratigraphy of the CESAR cores.- In: H.R. Jackson, P.J. Mudie & S.M. Blasko (eds), Initial Geological report on CESAR: The Canadian Expedition to Study the Alpha Ridge, Geol. Surv. Can. Pap. 84-22, 59-99.

Nam, S. (2009): Results of coarse fraction analysis.- In: W. Jokat (ed), The Expedition ARK-XXIII/3 of RV Polarstern in 2008, Rep. Pol. Mar. Res. 597: 53-58.

Nørgaard-Pedersen, N., Mikkelsen, N., Lassen, S.J., Kristoffersen, Y. & Sheldon, E. (2007a): Reduced sea ice concentrations in the Arctic Ocean during the last interglacial period revealed by sediment cores off northern Greenland. Paleoceanography 22: PA1218, doi:10.1029/2006PA001 283.

Nørgaard-Pedersen, N., Mikkelsen, N., Lassen, S.J. & Kristoffersen, Y. (2007b): Arctic Ocean record of last two glacial-interglacial cycles off North Greenland/Ellesmere Island - Implications for glacial history.- Mar. Geol. 244: 93-108.

Nørgaard-Pedersen, N., Spielhagen, R.F., Thiede, J. & Kassens, H. (1998): Central Arctic surface ocean environment during the past 80.000 years.- Paleoceanography 13: 193-204.

Nowaczyk, N.R., Antonow, M., Knies, J. & Spielhagen, R.F. (2003): Further rock magnetic and chronostratigraphic results on reversal excursions during the last 50 ka as derived from northern high latitudes and discrepancies in precise AMS14C dating.- Geophys. J. Internat. 155: 1065-1080.

Nowaczyk, N.R., Frederichs, T.W., Kassens, H., Norgaard-Pedersen, N., Spielhagen, R., Stein, R. & Weiel, D. (2001): Sedimentation rates in the Makarov Basin, central Arctic Ocean: a paleomagnetic and rock magnetic approach.- Paleoceanography 16: 368-389.

Nürnberg, D., Wollenburg, I., Dethleff, D., Eicken, H., Kassens, H., Letzig, T., Reimnitz, E. & Thiede, J. (1994): Sediments in Arctic sea ice: implications for entrainment, transport and release.- Mar. Geol. 119: 185-214.

O'Regan, M., King, J., Backman, J., Jakobsson, M., Pälike, H., Moran, K., Heil, C., Sakamoto, T., Cronin, T.M. & Jordan, R.W. (2008): Constraints on the Pleistocene chronology of sediments from the Lomonosov Ridge.- Paleoceanography 23: PA1S19, 1-18, doi:10.1029/2007PA001551.

Phillips, R.L. & Grantz, A. (1997): Quaternary history of sea ice and paleoclimate in the Amerasia Basin, Arctic Ocean, as recorded in the cyclical strata or Northwind Ridge.- Geol. Soc. Amer. Bull. 109: 1101-1115.

Phillips, R.L. & Grantz, A. (2001): Regional variations in provenance and abundance of ice-rafted clasts in Arctic Ocean sediments: implications for the configuration of Late Quaternary oceanic and atmospheric circulation in the Arctic.- Mar. Geol. 172: 91-115.

Polyak, L., Bischof, J., Ortiz, J.D., Darby, D.A., Channell, J.E.T., Xuan, C., Kaufman, D.S., Løvlie, R., Schneider, D.A., Eberl, D.D., Adler, R. & Council, E.A. (2009): Late Quaternary stratigraphy and sedimentpattern in the western Arctic Ocean.- Global Planet. Change XREF: doi:10.1016/j.gloplacha.2009.03.014.

Polyak, L., Edwards, M.H., Coakley, B.J. & Jakobsson, M. (2001): Ice shelves in the Pleistocene Arctic Ocean inferred from glaciogenic deep-sea bedforms.- Nature 410: 453-459.

Polyak, L.V., Curry, W.B., Darby, D.A., Bischof, J. & Cronin, T.M. (2004): Contrasting glacial/interglacial regimes in the western Arctic Ocean as exemplified by a sedimentary record from the Mendeleev Ridge.- Palaeogeogr. Palaeoclim. Palaeoecol. 203: 73-93.

Polyak, L.V., Darby, D.A., Bischoff, J.F. & Jakobsson, M. (2007): Stratigraphic constraints on late Pleistocene glacial erosion and deglaciation of the Chukchi margin, Arctic Ocean.- Quat. Res. 67: 234-245.

Proshutinsky, A.Y. & Johnson, M.A. (1997): Two circulation regimes of the wind-driven Arctic Ocean.- J. Geophys. Res. 102: 12493-12514.

Rachor, E. (ed) (1997): Scientific cruise report of the Arctic Expedition ARK-XI/1 of RV „Polarstern" in 1995.- Rep. Pol. Res. 226: 1-157.

Rothwell, R.G. (ed) (2006): New techniques in sediment core analysis.- Geol Soc. London Spec. Publ. 267: 1-266.

Schauer, U. (ed), 2008. The expedition ARKXXII-2 of the Research Vessel "Polarstern" in 2007 – a contribution to the International Polar Year 2007/08. Rep Pol. Mar. Res., in press.

Schreck, M., Bazhenova, E., Eckert, S., März, C., Matthiessen, J. & Stein, R. (2009): Colour logging.- In: W. JOKAT (ed) (2009): The Expedition ARK-XXIII/3 of RV Polarstern in 2008, Rep. Pol. Mar. Res. 597: 27-29

Schulte-Loh, I. (2009): Paläoumweltbedingungen im spätquartären Arktischen Ozean: Rekonstruktion nach sedimentologischen Untersuchungen an Sedimentkernen vom Mendeleev-Rücken.- Unpubl. Master Thesis, Bremen University.

Scott, D.B., Mudie, P.J., Baki, V., MacKinnon, K.D. & Cole, F.E. (1989): Biostratigraphy and Late Cenozoic paleoceanography of the Arctic Ocean: foraminiferal, lithostratigraphic, and isotopic evidence.- Geol. Soc. Amer. Bull. 101: 260-277.

Sellén, E., Jakobsson, M. & Backman, J. (2008): Sedimentary regimes in Arctic's Amerasian and Eurasian Basins: clues to differences in sedimentation rates.- Global Planet. Change 61: 275-284.

Serreze, M.C., Walsh, J.E., Chapin, F.S., Osterkamp, T., Dyurgerov, M., Romanovsky, V., Oechel, W.C., Morison, J., Zhang, T. & Barry, R.G. (2000): Observational evidence of recent change in the northern high-latitude environment.- Clim. Change 46: 159-207.

Shackleton, N.J. (1987): Oxygen isotopes, ice volume and sea level.- Quat. Sci. Rev. 6: 183-190.

Spielhagen, R.F., Baumann, K.-H., Erlenkeuser, H., Nowaczyk, N.R., Nørgaard-Pedersen, N., Vogt, C. & Weiel, D. (2004): Arctic Ocean deep-sea record of Northern Eurasian ice sheet history.- Quat. Sci. Rev. 23: 1455-1483.

Spielhagen, R.F., Bonani, G., Eisenhauer, A., Frank, M., Frederichs, T., Kassens, H., Kubik, P.W., Mangini, A., Nörgaard-Pedersen, N., Nowaczyk, N.R., Schäper, S., Stein, R., Thiede, J., Tiedemann, R. & Wahsner, M. (1997): Arctic Ocean evidence for Late Quaternary initiation of northern Eurasian ice sheets.- Geology 25: 783-786.

Stein, R. (ed) (2005): Scientific cruise report of the Arctic Expedition ARK-XX/3 of RV "Polarstern" in 2004: Fram Strait, Yermak Plateau and East Greenland continental margin.- Rep. Pol. Mar. Res. 517: 1-188.

Stein, R. (2008): Arctic Ocean Sediments: Processes, Proxies, and Palaeoenvironment.- Elsevier, Amsterdam, Developments in Marine Geology 2: 1-587.

Stein, R., Behrends, M., Bourtman, M., Fahl, K., Mitjajev, M., Musatov, E., Niessen, F., Nørgaard-Pedersen, N., Shevchenko, V. & Spielhagen, R. (1997): Marine-geological investigations, „Polarstern" Expedition ARK-XI/1.- In: E. RACHOR (ed) Scientific cruise report of the Arctic Expedition ARK-XI/1 of RV „Polarstern" in 1995.- Rep. Pol. Res. 226: 117-154.

Stein, R., Boucsein, B., Fahl, K., Garcia de Oteyza, T., Knies, J. & Niessen, F. (2001): Accumulation of particulate organic carbon at the Eurasian continental margin during late Quaternary times: controlling mechanisms and paleoenvironmental significance.- Global Planet. Change 31: 87-102.

Stein, R., Grobe, H. & Wahsner, M. (1994a): Organic carbon, carbonate, and clay mineral distributions in eastern central Arctic Ocean surface sediments.- Mar. Geol. 119: 269-285.

Stein, R., Hefter, J., Grützner, J., Voelker, A. & Naafs, B.D.A. (2009a): Variability of surface-water characteristics and Heinrich Events in the Pleistocene mid-latitude North Atlantic Ocean: Biomarker and XRD records from IODP Site U1313 (MIS 16-9).- Paleocanography 24: PA2203, doi:10.1029/2008PA001639.

Stein, R., Krylov, A., Matthiessen, J., Nam, S., Niessen, F. & the ARK-XXIII/3 Geology Group (2009b): Main lithologies and lithostratigraphy of ARK-XXIII/3 sediment cores.- In: W. JOKAT (ed), The Expedition ARK-XXIII/3 of RV Polarstern in 2008.- Rep. Pol. Mar. Res. 597: 12-86.

Stein, R., Kukina, N., Matthiessen, J., Müller, C., Nørgaard-Pedersen, N. & Usbeck, R. (1999): Lithostratigraphy of Alpha Ridge sediments cores.- In: W. JOKAT (ed), Arctic'98: The Expedition ARKXIV/1a of RV Polarstern in 1998, Rep. Pol. Res. 308: 60-75.

Stein, R., Matthiessen, J. & Niessen, F. (2010): Re-coring at Ice Island T3 site of key core FL-224 (Nautilus Basin, Amerasian Arctic): sediment characteristics and stratigrraphic framework.- Polarforschung 79(2): 81-96.

Stein, R., Nam, S.-I., Schubert, C., Vogt, C., Fütterer, D. & Heinemeier, J. (1994b): The last deglaciation event in the eastern central Arctic Ocean.- Science 264: 692-696.

Stein, R., Schubert, C.J., Vogt, C. & Fütterer, D. (1994c): Stable isotope stratigraphy, sedimentation rates, and salinity changes in the Latest Pleistocene to Holocene eastern central Arctic Ocean.- Mar. Geol. 119: 333-355.

Steuerwald, B.A., Clark, D.L. & Andrew, J.A. (1968): Magnetic stratigraphy and faunal patterns in Arctic Ocean sediments.- Earth Planet. Sci. Lett. 5: 79-85.

Stokes, C.R., Clark, C.D., Darby, D.A. & Hodgson, D.A. (2005): Late Pleistocene ice export events into the Arctic Ocean from M'Clure Strait Ice Stream, Canadian Arctic Archipelago.- Global Planet. Change 49: 139-162.

Svendsen, J.I., Alexanderson, H., Astakhov, V.I., Demidov, I., Dowdeswell, J.A., Funder, S., Gataullin, V., Henriksen, M., Hjort, C., Houmark-Nielsen, M., Hubberten, H.-W., Ingólfsson, O., Jakobsson, M., Kjær, K.H., Larsen, E., Lokrantz, H., Lunkka, J.P., Lyså, A., Mangerud, J., Matioushkov, A., Murray, A., Möller, P., Niessen, F., Nikolskaya, O., Polyak, L., Saarnisto, M., Siegert, C., Siegert, M.J., Spielhagen, R.F. & Stein, R. (2004): Late Quaternary ice sheet history of Northern Eurasia.- Quat. Sci. Rev. 23: 1229-1272.

Thompson, D.W.J. & Wallace, J. M. (1998): The Arctic Oscillation signature in the wintertime geopotential height and temperature fields.- Geophys. Res. Lett. 25: 1297-1300.

Thompson, W.G. & Goldstein, S.L. (2006): A radiometric calibration of the SPECMAP timescale.- Quat. Sci. Rev. 25: 3207-3215.

Viscosi, S., Mammone, K., Pisias, N., & Dymond, J. (2003): Clay mineralogy and multi-element chemistry of surface sediments on the Siberian-Arctic shelf: implications for sediment provenance and grain size sorting.- Cont. Shelf Res. 23: 1175-1200.

Vogt, C. (1997): Regional and temporal variations of mineral assemblages in Arctic Ocean sediments as climatic indicator during glacial/interglacial changes.- Rep. Pol. Res. 251: 1-309.

Wahsner, M., Müller, C., Stein, R., Ivanov, G., Levitan, M., Shelekova, E. & Tarasov, G. (1999): Clay mineral distributions in surface sediments from the Central Arctic Ocean and the Eurasian continental margin as indicator for source areas and transport pathways: a synthesis.- Boreas 28: 215-233.

Weber, M.E., Niessen, F., Kuhn, G. & Wiedicke, M. (1997): Calibration and application of marine sedimentary physical properties using a multi-sensor core logger.- Mar. Geol. 136: 151-172.

Wheeler, P.A. (ed) (1997): 1994 Arctic Ocean section.- Deep-Sea Res II 44: 1483-1757.